Preparation, characterization and catalytic activity of Ni NPs supported on porous alginate-g-poly(*p*-styrene sulfonamide-*co*-acrylamide)

Sedigheh Alavinia, Ramin Ghorbani-Vaghei*

Department of Organic Chemistry, Faculty of Chemistry, Bu-Ali Sina University, 6517838683, Hamadan, Iran

***Corresponding author; E-mail: rgvaghei@yahoo.com and ghorbani@basu.ac.ir; Tel: +98(81)38380647**

1. Experimental

All commercially available chemicals were obtained from Merck and Fluka companies and used without further purification otherwise stated. Nuclear magnetic resonance (NMR) spectra were recorded in $CDCl_3$ on Bruker Avance spectrometers 250 and 500 MHz for ^1H NMR and 63 and 125 MHz for ^{13}C NMR using TMS as an internal standard; chemical shifts were expressed in parts per million (ppm). Infrared (IR) spectroscopy was conducted on a Perkin Elmer GX FT-IR spectrometer. Mass spectra were recorded on a Shimadzu QP 1100 BX Mass Spectrometer. Melting points were determined on a Stuarf Scientific SMP3 apparatus. Powder X-ray diffraction (PXRD) patterns recorded on a Rigaku XDS 2000 diffractometer using nickel-filtered CuKa radiation (λ =1.5418) over a range of <50_. Thermo-gravimetric analysis (TGA) was performed on a PYRIS DIAMOND instrument. Inductively coupled plasma-atomic emission spectroscopy (ICP-AES) was conducted on a Varian Vista MPX ICPAES instrument. The qualitative analysis of Alg-PSSA-*co*-ACA@Ni was performed by using energy dispersive was performed by using energydispersive X-ray spectroscopy (EDS). Scanning electron microscopy (SEM) was performed on EM3200 instrument operated at 30 kV accelerating voltage. Transmission electron microscopy (TEM) was performed using a Zeiss-EM10C-100kv. Prior to the surface area analysis, the samples were activated in a high vacuum at 80 ^{0}C for12 hr. All adsorption and desorption measurements were performed on a Micromeritics TriStar 3020 version 3.02 (N_2) system and measured at 77 K. The data were analyzed using the TriStar II 3020 V1.03 software (Micromeritics, Norcross, GA). The pore size distributions were calculated from the adsorption–desorption isotherms. Wavelength-dispersive X-ray spectroscopy (WDX) was performed using a TESCAN mira3.

1.1. Synthesis of silica alginate-g-poly (*p*-styrene sulfonamide-*co*-acrylamide) (SiO_2@Alg-PSSA-*co*-ACA).

silica NPs was synthesized through the Stöber method.[1] Then, the mixture of *p*-Styrene sulfonamide (1.5 g), MBA (0.2 g) and SiO_2 NPs (0.05 g) was gradually added to the sodium alginate solution (0.5 g in 20 mL distilled water). Finally, ammonium persulfate (APS) (0.6 g) was added and the mixture stirred at 60 ^{0}C for 2 h. The synthesized SiO_2@Alg-PSSA-*co*-ACA nanocomposite, in the form of gel, was dried at room temperature (weight: 5 g).

1.2. Synthesis of porous alginate-g-poly(styrene sulfonamide-*co*-acrylamide) (Alg-PSSA-*co*-ACA).

In order to synthesize mesoporous structure, SiO_2 NPs of SiO_2@Alg-PSSA-*co*-ACA were selectively removed through etching silica NPs by mixing HF solution (5 mL, 10 wt%) to the solution of SiO_2@Alg-PSSA-*co*-ACA (1 g in 20 mL deionized water) in a plastic tube. The prepared solution was stirred for 3 h. The resultant porous Alg-PSSA-*co*-ACA was separated by filtration, washed with water, and dried (weight: 0.85 g).

1.3. Nickel nanoparticles immobilized on porous alginate-g-poly (*p*-styrene sulfonamide-*co*-acrylamide) (Alg-PSSA-*co*-ACA@Ni).

To synthesize the Alg-PSSA-*co*-ACA@Ni, the obtained porous Alg-PSSA-*co*-ACA (0.1 g) in the solution of $NiCl_2$-$6H_2O$ (1 M, 5 mL) was stirred at room temperature for 2h, then the solution of $NaBH_4$ (10 mmol in 5 mL ethanol) was slowly added and stirred at room temperature for 60 min. The functionalized Alg-PSSA-*co*-ACA@Ni was separated with centrifusion, washed with distilled water (3 x 20 mL), and dried under vacuum conditions at room temperature for 12 h (weight: 0.3 g) (Scheme 1).[2] The amount of Ni incorporated in the support was 1.6 mmol g^{-1}, as corroborated by ICP-OES.

1.4. General procedure for the synthesis of 1,3,4-oxadiazoles.

A mixture of substituted benzohydrazide (1 mmol), substituted aryl iodide (1 mmol), $KHCO_3$ (1 mmol), *tert*-butyl isocyanide (1.5 mmol), and Alg-PSSA-*co*-ACA@Ni (1.5 mol%, 9 mg) was refluxed in H_2O:EtOH (2 mL, 1:1). After the completion of the reaction (by TLC :*n*-hexane/ethyl acetate, 10:4), the catalyst was separated from the reaction mixture by centrifution, washed with ethanol (10 mL). Finally, the solvent of the reaction was evaporated and the solid obtained were crystallized from ethanol (10 mL). In some cases, the residue was purified by a short silica gel column *n*-hexane/ethylacetate (10:4).

2. Results and discussions

2.1. Catalyst characterization

The synthesized Alg-PSSA-*co*-ACA@Ni catalyst was fully characterized by FT-IR, TGA, ICP-MS, FESEM-EDX mapping techniques and N_2 isotherms. The FT-IR spectrum of sodium alginate, SiO_2@Alg-PSSA-*co*-ACA, mesoporous Alg-PSSA-*co*-ACA, and Alg-PSSA-*co*-ACA@Ni is shown in Fig. 1. The results obtained from FT-IR spectrum show that: (I) the presence of SiO_2 NPs template, (II) the polymerization of PSSA and crosslinking of MBA groups (III) selective removal of the SiO_2 NPs from SiO_2@Alg-PSSA-*co*-ACA (IV) the interaction of Ni NPs with the prepared support. FT-IR spectrum of NaAlg displayed vibration bands at 1642 and 1454 cm^{-1} (due to vibrations of carboxylate anions). The vibration bands at 3412 cm^{-1} and 2929.87 cm^{-1} can be attributed to the O-H and C-H stretching, respectively (Fig. 1A). The FT-IR spectrum of SiO_2@Alg-PSSA-*co*-ACA displayed new bands at 3363,

3090 and 1662 cm^{-1} can be related to O-H, C-H and C=O amide stretching bands, respectively. The presence of these peaks confirmed successful crosslinking of MBA. In addition, the presence of new bands at 1328 and 1159 cm^{-1} (due to the O=S=O stretching) was confirmed the successful polymerization of PSSA .[3] Also, the peaks at 1180 cm^{-1} approved the SiO_2 NPs presence (Fig. 1B).[4] After silica etching procedure, this peak was not observed in the FT-IR spectra of the porous Alg-PSSA-*co*-ACA and Alg-PBSA-*co*-ACA@Ni (Figs. 1C and 1D). In the FT-IR spectrum of Alg-PSSA-*co*-ACA@Ni (Fig. 1D), after interaction of Ni NPs with prepared support, the band at 3392 cm^{-1} (due to the NH_2 stretching, Fig. 3C) shifted to lower wave number (3363 cm^{-1}). In addition, the amide peaks shifted from 1633 cm^{-1} to 1600 cm^{-1}. Based on the strong co-ordination of Ni NPs with the composite, the IR absorption peaks of the organo-functions are slightly shifted to lower regions.

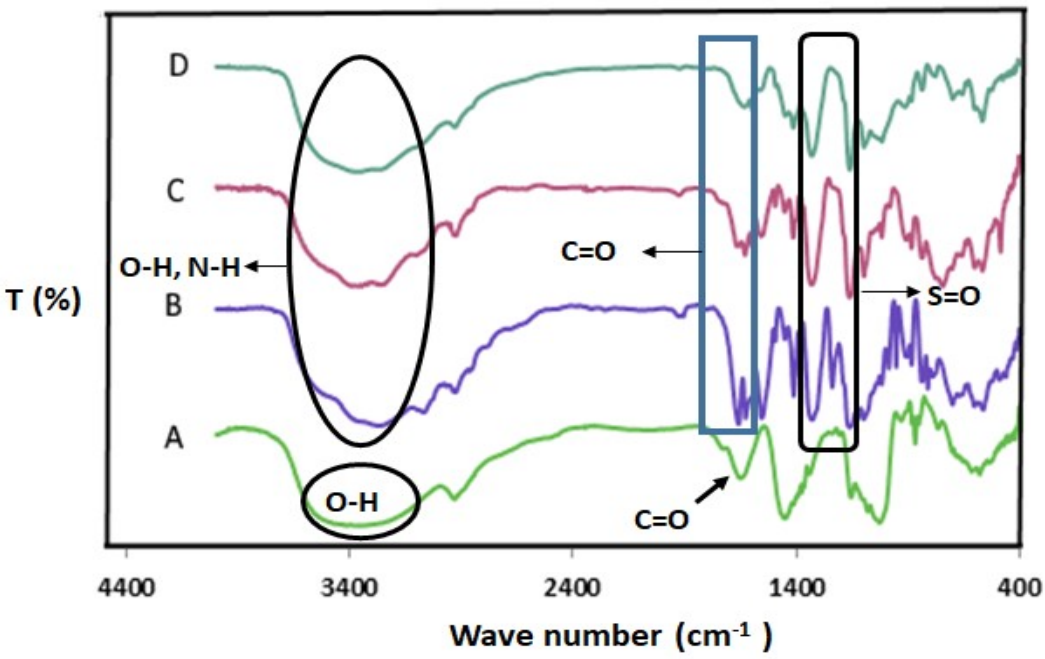

Fig. 1. FT-IR spectra of NaAlg (A), SiO_2@Alg-PBSA-*co*-ACA (B), Porous Alg-PSSA-*co*-ACA (C), Alg-PSSA-*co*-ACA@Ni (D).

Figure 2 shows the X-ray diffraction pattern of the Porous Alg-PSSA-co-ACA@Ni samples before (Fig. 2A) and after the reaction (Fig. 2B). Comparison of X-ray diffraction patterns of Alg-PSSA-co-ACA@Ni sample shows that the structure of prepared catalyst has not changed much after the reaction. The diffraction peaks appeared at 2θ=60° can be attributed to the Ni nanoparticles.[5] Meanwhile, in the X-ray diffraction pattern of the Alg-PSSA-co-ACA@Ni nanocomposite sample, an amorphous phase is observed, which is related to the presence of amorphous polymer filaments of acrylamide (2θ=20-30 degrees) [6], and sodium alginate (2θ=35-40 degrees) [7], and polystyrene sulfonamide (2θ=20-30 degrees).[8] It is noteworthy

that the crystal structure of the recovered catalyst sample is quite similar to that of the original catalyst structure only the peak positions of the appeared peaks has a bit changed., indicating the stability of the recovered catalyst. Therefore, the prepared catalyst can be used several times after a simple recovery period.

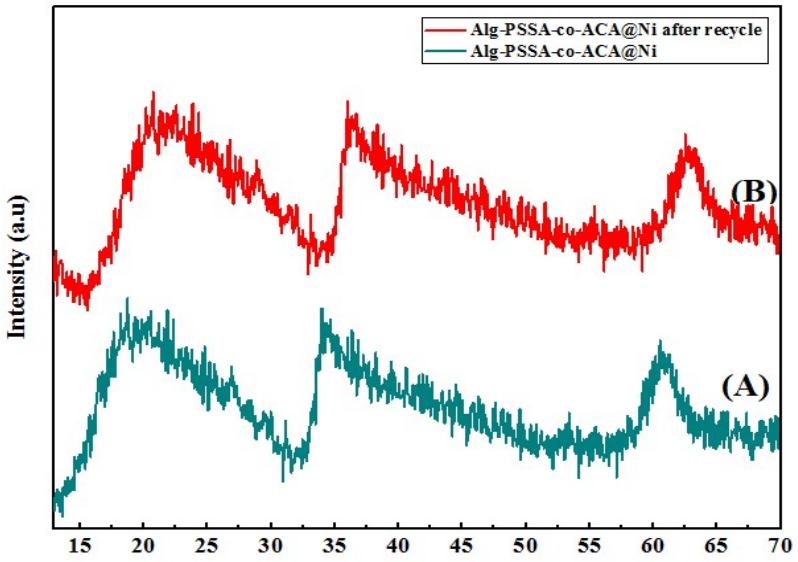

Fig. 2. XRD pattern of porous Alg-PSSA-co-ACA@Ni before (A) and after the reaction (B).

The morphology of SiO_2 nanoparticles, mesoporous Alg-PSSA-*co*-ACA and Alg-PSSA-*co*-ACA@Ni was characterized with FE-SEM analysis (Fig. 3). The FE-SEM of spherical SiO_2 NPs showed a uniform distribution (Fig. 3A). FE-SEM image of Alg-PSSA-*co*-ACA that obtained from silica template method demonstrated the mesoporous structure of Alg-PSSA-*co*-ACA (Fig. 3B). Fig. 3B shows the rough morphology of the surface which causes more activity of catalyst. Fig. 3C and Fig. 3D showed the distribution of spherical shaped Ni particles on the surface of mesoporous Alg-PSSA-*co*-ACA.

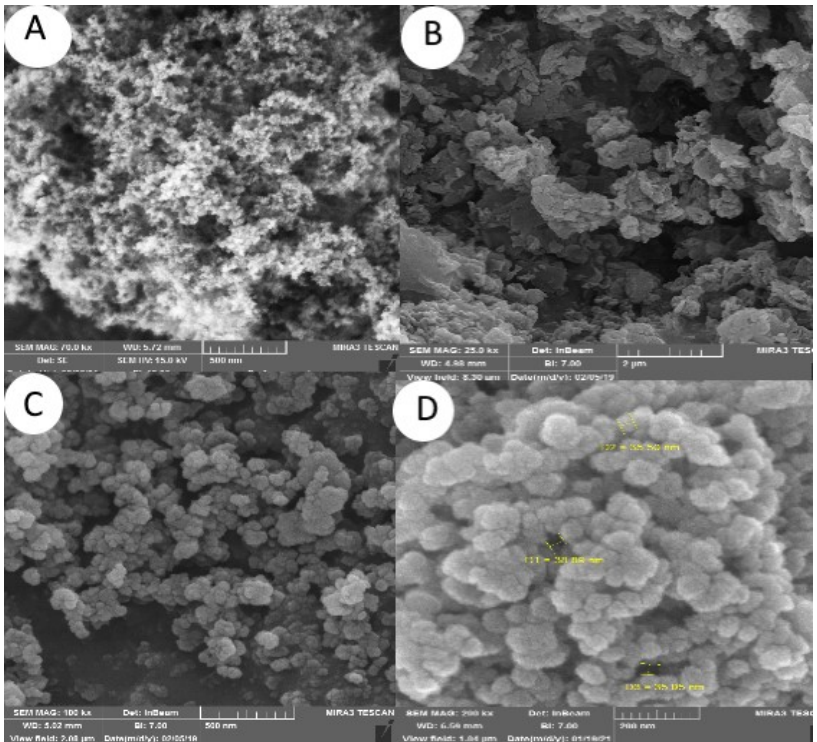

Fig. 3. FE-SEM photographs of SiO_2NPs (A), mesoporous Alg-PSSA-*co*-ACA (B), mesoporous Alg-PSSA-*co*-ACA@Ni (C-D).

HR-TEM images of Alg-PSSA-*co*-ACA@Ni (Fig. 4A) and recovered catalyst (Fig. 4B) are depicted in Fig. 4. HR-TEM images showed that the sample has uniform ~20 nm particles. Good dispersion of Ni species was visible in higher magnifications HR-TEM image, a very thin layer of porous polymer could be detected around the Ni NPs. In the prepared catalyst, the porous Alg-PSSA-*co*-ACA can play the roles of both reducing and capping agents. In addition, deposition of Ni NPs was verified by the means of EDX. HR-TEM image demonstrated the presence of Ni NPs along with polymer in the catalyst without any noticeable change compare with the original one. In comparison with the fresh particles (Fig. 4A), the number of the Ni NPs distributed on the mesoporous Alg-PSSA-*co*-ACA substrate seems to be reduced. It may be a reason for the observed reduction in the catalytic performance after 7-time recycling. To obtain more confirmation on this claim, the inductively coupled plasma optical emission spectroscopy (ICP-OES) was performed on a sample of the supernatant after seventh time of the particles usage, and it was revealed that 1.55 mmolg-1 of Ni element exist in the sample. It means that the leaching of the Ni element from the catalytic system is an inevitable event, but this partial leaching does not have any significant effects on the catalytic performance.

.

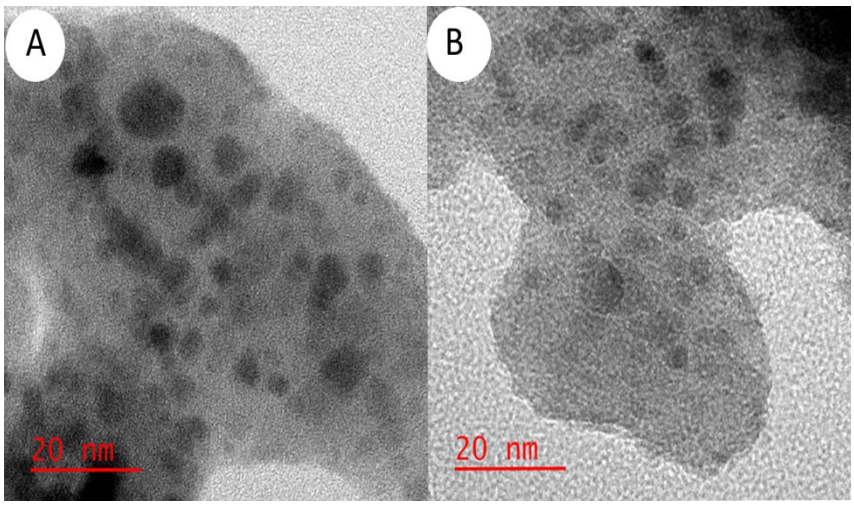

Fig. 4. HR-TEM photographs of mesoporous Alg-PSSA-*co*-ACA@Ni before (A) and after the reaction (B).

The elemental composition of the Alg-PSSA-*co*-ACA@Ni was determined by EDS analysis and presence of (Na, O, S, C, N and, Ni) was confirmed (Fig. 5). From the weight percentage results of the EDS analysis of the prepared catalyst (Table 1), it can be understood that the successful polymerization of *para*-styrene sulfonamide (S: 30.41%). The presence of the N (9.28%) and O (26.10) also confirmed the

crosslinking of MBA and the polymerization of PSSA (Table 1). In addition, elemental mapping exhibited the uniform distribution of all the elements, as shown in Fig. 6. In addition, proper dispersion of Ni NPs is obvious, in the composite.

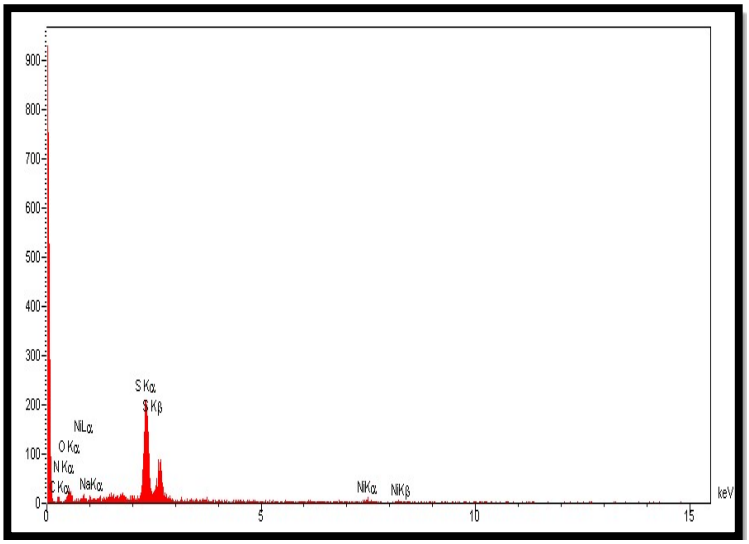

Fig. 5. EDX spectrum of Alg-PSSA-*co*-ACA@Ni.

Table 1. Elemental percentage of Alg-PSSA-*co*-ACA@Ni.

Element	W%	A%
C	28.34	42.36
N	9.28	6.76
O	26.10	29.28
Na	1.13	0.88
S	30.41	19.27
Ni	4.74	1.45
Totals	100.0	

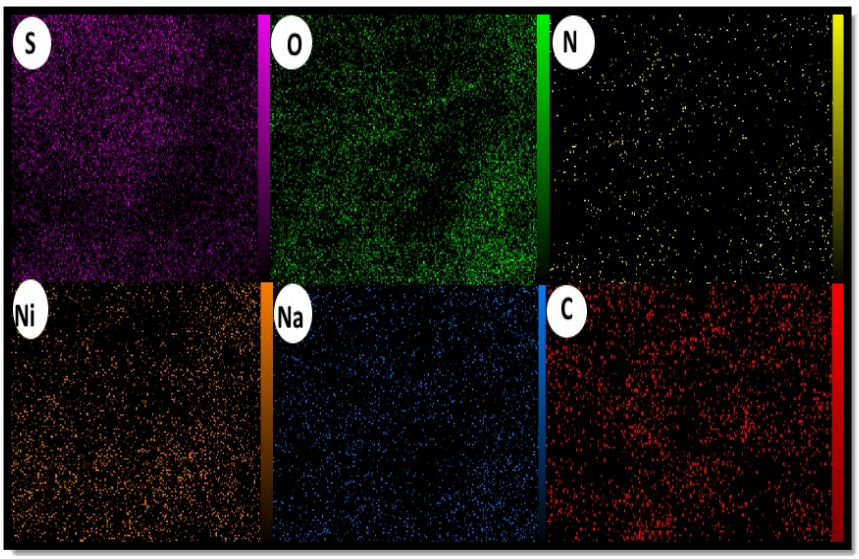

Fig. 6. Elemental mapping of the C, N, O, S, Ni and Na atoms achieved from SEM micrographs.

Fig. 7 shows the TGA curve of Alg-PSSA-*co*-ACA@Ni in which a small weight loss from 30 to 100 ℃ was witnessed, clearly related to the physically absorbed water. After this, the weight loss in the range of 230−320 ℃ clearly indicated the degradation of Alg-PSSA-*co*-ACA groups.[9]

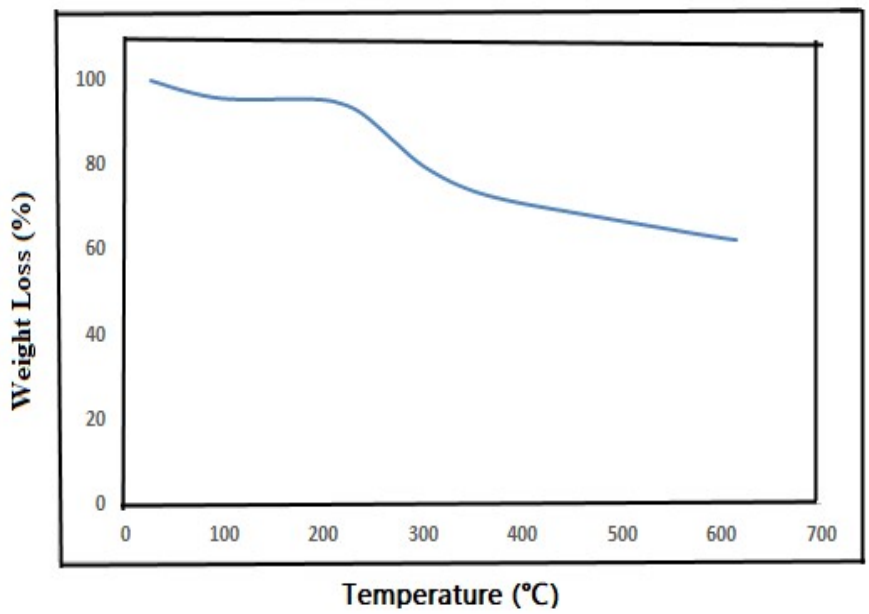

Fig. 7. TGA curve of Alg-PSSA-*co*-ACA@Ni.

As shown in Fig. 8, according to the Brunauer–Emmett–Teller (BET) analysis, Alg-PSSA-*co*-ACA (Fig. 8A) and Alg-PSSA-*co*-ACA@Ni (Fig. 8B) indicated a typical type IV isotherm with type H3 hysteresis (defined by IUPAC).[10] The results of N_2-adsorption and desorption isotherms of Alg-PSSA-*co*-ACA and Alg-PSSA-*co*-ACA@Ni clearly demonstrated the immobilization of Ni NPs significantly reduces the pore diameter, pore volume and specific surface area (Table 2).

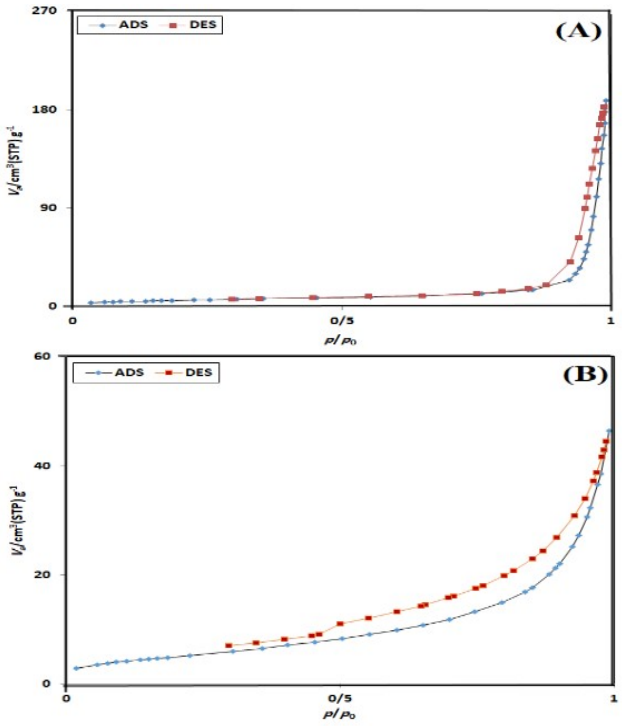

Fig. 8. N_2 adsorption–desorption isotherms of porous Alg-PSSA-*co*-ACA (A) and Alg-PSSA-*co*-ACA@Ni (B).

Table 2. Texture parameters obtained from nitrogen adsorption studies.

Sample	SBET (m^2g^{-1})	Pore diameter by BJH method (nm)	Pore volume (cm^3g^{-1})
Alg-PSSA-*co*-ACA	22.41	25.55	0.27
Alg-PSSA-*co*-ACA@Ni	21.30	1.88	0.07

The N_2 adsorption-desorption isotherms of the 7th reused catalyst (Fig. 9) were measured in order to determine the textural properties. It can be seen from Fig. 9 that reused catalyst indicate a typical type IV isotherm with type H3 hysteresis (defined by IUPAC), which are identified as mesoporous material.[10]
The N_2 adsorption-desorption isotherms of reused catalyst indicates that there was no obvious change for the catalyst composition after the reaction. The changes associated to the textural properties of the 7th reused catalyst can be due to the fact that reactants which were distributed inside the Alg-PSSA-*co*-ACA@Ni pores during the reaction (Pore volume = 0.05 cm^3g^{-1}, SBET= 6.41 m^2g^{-1}).

References:

[1] W. Stöberand, A. Fink, *J. Colloid. Interf. Sci*. 1968, **26**, 62-69.
[2] S. Khan, A. Ghatak, S. Bhar, *Tetrahedron Lett*. 2015, **56**, 2480-2487.
[3] A. G. Ibrahim, A. Z. Sayed, H. A. El-Wahab, M. M. Sayah, *Am. J. Polym. Sci. Technol.* 2019, **5**, 55-62.
[4] J. Lin, H. Huang, M. Wang, J. Deng, *Polym. Chem*. 2016, **7**, 1675-1681.

[5] M.R. Ahghari, V. Soltaninejad, A. Maleki, *Sci. Rep*. 2020, **28**, 1-0.

[6] T.A. Saleh, A.M. Elsharif, S. Asiri, A.R. Mohammed, H. Dafalla. *Environ. Nanotechnol. Monit. Manag.* 2020, **14**, 100302.

[7] A. Ahmed, F. Mohamed, A.M. Elzanaty, O.F. Abdel-Gawad *Int. J. Biol. Macromol*. 2021, **167**, 766-776.

[8] L. Jia , D. Wang , L. Liu , S. Zhang , T. Xu , *Des Monomers Polym*, 2014, **17**, 425–429 .

[9] Z. Bahrami, A. Akbari, B. Eftekhari-Sis, *Int. J. Biol. Macromol*. 2019, **129**, 187–197.

[10] S.W. Sing, W. Kenneth, *Adsorp. Sci. Technol*. 2004, **22**, 773-782.

Fig.9. N_2 adsorption–desorption isotherms of the recovered Alg-PSSA-*co*-ACA@Ni.

Preparation, characterization and catalytic activity of Ni NPs supported on porous alginate-g-poly(*p*-styrene sulfonamide-*co*-acrylamide)

Sedigheh Alavinia, Ramin Ghorbani-Vaghei*

Department of Organic Chemistry, Faculty of Chemistry, Bu-Ali Sina University, 6517838683, Hamadan, Iran

*Corresponding author; E-mail: rgvaghei@yahoo.com and ghorbani@basu.ac.ir; Tel: +98(81)38380647

Spectra Data:

2-(2-Bromophenyl)-5-phenyl-1,3,4-oxadiazole.

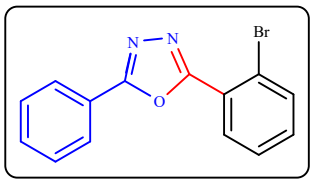

The general procedure was followed. Purification by column chromatography (silica gel, *n*-hexan/EtOAc, 10:3) gave the desired product as a yellow solid. M.p. 148–150°C,[1] M.p. 145–147°C, 1H NMR (500 MHz, CDCl3-*d*3) δ 6.83 (d, 2H, *J* = 8 Hz), 6.94 (t, 1H, *J* = 7.2 Hz), 7.30 (dd, 3H, *J* = 7.6, 5.6 Hz), 7.45 (t, 1H, *J* = 7.6 Hz), 7.69 (d, 1H, *J* = 7.6 Hz), 7.80 (dd, 1H, *J* = 6.4, 1.2 Hz);. ^{13}C NMR (125 MHz, DMSO-d_6) δ 164.7, 163.2, 135.1, 132.6, 132.4, 132.1, 129.8, 129.4, 127.2, 127.1, 126.1, 123.6, 122.9. MS *m/z*: 299.1

2-(2-Chlorophenyl)-5-(pyridin-4-yl)-1,3,4-oxadiazole.

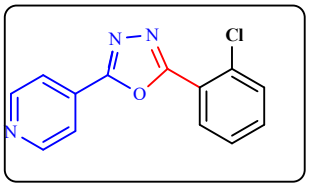

The general procedure was followed. Purification by column chromatography (silica gel, *n*-hexan/EtOAc, 10:3) gave the desired product as a yellow solid. M.p. 128–130 °C,[2] ^{1}H NMR (500 MHz, DMSO-d_6) δ 8.85 (d, *J* = 4.8 Hz, 1H), 8.16 (d, *J* = 2.8 Hz, 1H), 8.12 – 8.03 (m, 2H), 7.87 (d, *J* = 5.5 Hz, 1H), 7.72 (dd, *J* = 8.1, 2.4 Hz, 1H), 7.65 (qd, *J* = 8.0, 7.5, 2.7 Hz, 1H), 7.51 (td, *J* = 8.0, 3.1 Hz, 1H). ^{13}C NMR (125 MHz, DMSO-d_6) δ 164.1, 163.3, 151.3, 134.6, 133.7, 133.3, 132.6, 131.9, 131.0, 130.7, 129.2, 128.3, 126.9, 126.0, 125.4, 120.8, MS *m/z*: 257.1

2-(5-Phenyl-1,3,4-oxadiazol-2-yl) benzaldehyde.

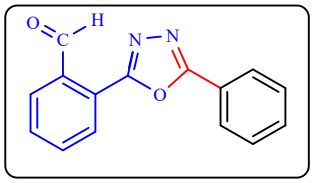

The general procedure was followed. Purification by column chromatography (silica gel, *n*-hexan/EtOAc, 10:3) gave the desired product as a yellow solid. M.p. 180–181 °C; ^{1}H NMR (500 MHz, DMSO-d_6) δ ^{1}H NMR (500 MHz, DMSO-d_6) δ 6.85 (d, 2H, *J*=8.4 Hz), 7.19 (t, 2H, *J*= 7.6 Hz), 7.44 (d, 1H, 4.8 Hz), 7.49 (dd, 2H, *J*=7.6, 7.2 Hz), 7.61 (d, 2H, *J*=7.2 Hz); 8.88 (s, 1H). ^{13}C NMR (125 MHz, DMSO-d_6) δ, 169.2, 160.1, 147.4, 146.8, 138.7, 134.8, 134.7, 134.1, 132.3, 132.2, 130.8, 130.4, 129.5, 128.0, 127.6, 127.2, 125.8, 125.0, 124.8, 124.5, 124.4, 124.1, 122.7. MS *m/z*: 250.07

2-(3-Chlorophenyl)-5-phenyl-1,3,4-oxadiazole.

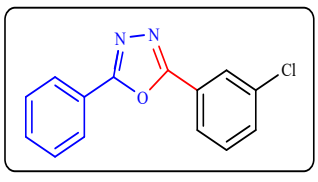

The general procedure was followed. Purification by column chromatography (silica gel, *n*-hexan/EtOAc, 10:3) gave the desired product as a white solid. M.p. 119–121 °C;[3] ^{1}H NMR (250 MHz, DMSO-d_6) δ 8.07-8.20 (m, 4H), 7.57-7.73 (m, 5H). MS *m/z*: 257.04

2-(3-Chlorophenyl)-5-(pyridin-4-yl)-1,3,4-oxadiazole.

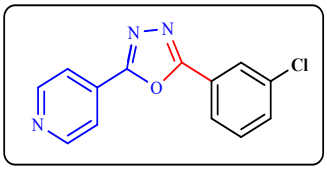

The general procedure was followed. Purification by column chromatography (silica gel, *n*-hexan/EtOAc, 10:3) gave the desired product as a white solid. M.p. 143–145°C;[4] ^{1}H NMR (250 MHz, DMSO-*d*6) δ 8.85 (s, 2H), 8.19 (s, 1H), 8.10 (s, 3H), 7.69 (dq, *J* = 14.7, 7.7 Hz, 2H). ^{13}C NMR (63 MHz, DMSO-d_6) δ 164.1, 163.2, 151.3, 134.5, 132.6, 131.9, 130.7, 126.9, 126.0, 125.3, 121.0. MS *m/z*: 257.6.

2-(4-Bromophenyl)-5-methyl-1,3,4-oxadiazole.

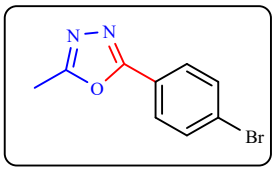

The general procedure was followed. Purification by column chromatography (silica gel, *n*-hexan/EtOAc, 10:3) gave the desired product as a yellow solid. M.p. 110–112 °C;[5] ^{1}H NMR (250 MHz, DMSO-d_6) δ 8.06 (d, *J* = 8.2 Hz, 2H), 7.83 (d, *J* = 8.2 Hz, 2H), 2.56 (s, 3H). MS *m/z*: 237.9.

2-Benzyl-5-phenyl-1,3,4-oxadiazole.

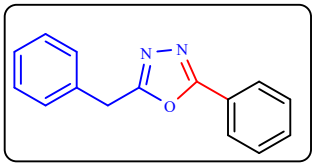

The general procedure was followed. Purification by column chromatography (silica gel, *n*-hexan/EtOAc, 10:3) gave the desired product as a yellow solid. M.p. 102–103 °C;[6] ^{1}H NMR (250 MHz, DMSO-d_6) δ 7.93 (d, *J* = 6.9 Hz, 2H), 7.56 (d, *J* = 6.2 Hz, 4H), 7.36 (d, *J* = 4.4 Hz, 4H), 4.34 (s, 2H). ^{13}C NMR (63 MHz, DMSO-d_6) δ 165.9, 164.6, 134.8, 132.2, 129.7, 129.2, 127.6, 126.7, 123.7, 31.2. MS *m/z*: 236.2.

2-(4-Bromophenyl)-5-phenyl-1,3,4-oxadiazole.

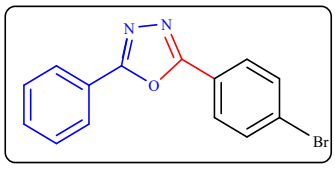

The general procedure was followed. Purification by recrystallization with EtOH gave the desired product as a white solid. M.p. 165–166 °C;[1]^{1}H NMR (250 MHz, DMSO-d_6) δ 8.18 – 7.97 (m, 3H), 7.83 (d, *J* = 7.2 Hz, 3H), 7.71 – 7.55 (m, 3H). ^{13}C NMR (63 MHz, DMSO-d_6) δ 164.8, 163.8, 132.9, 132.5, 129.8, 129.0, 127.7, 126.1, 123.6, 122.9.

4-(5-Phenyl-1,3,4-oxadiazol-2-yl) aniline.

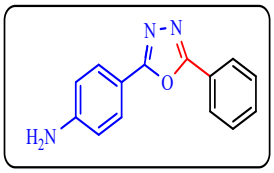

The general procedure was followed. Purification by column chromatography (silica gel, *n*-hexan/EtOAc, 10:3) gave the desired product as a yellow solid. M.p. 191–193 °C;[7] ^{1}H NMR (250 MHz, DMSO-d_6) δ 8.18 – 7.98 (m, 2H), 7.75 (d, J = 8.2 Hz, 2H), 7.58 (s, 3H), 6.69 (d, J = 8.2 Hz, 2H), 5.98 (s, 1H). ^{13}C NMR (63 MHz, DMSO) δ 165.2, 163.0, 152.9, 131.9, 129.7, 128.9, 128.6, 127.9, 126.7, 124.1, 114.0, 110.0. MS *m/z*: 237.2.

2-Benzyl-5-(p-tolyl)-1,3,4-oxadiazole.

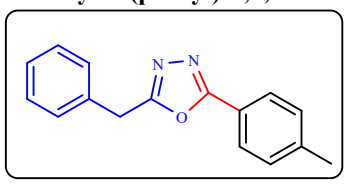

The general procedure was followed. Purification by column chromatography (silica gel, *n*-hexan/EtOAc, 10:3) gave the desired product as a white solid. M.p. 93-94 °C;[8] ^{1}H NMR (250 MHz, DMSO-d_6) δ 7.79 (d, J = 7.8 Hz, 2H), 7.61 – 6.96 (m, 7H), 4.31 (s, 2H), 2.48 (s, 3H). ^{13}C NMR (63 MHz, DMSO-d_6) δ 165.6, 164.7, 142.3, 136.2, 134.9, 130.3, 129.7, 129.5, 129.3, 129.1, 128.6, 127.9, 127.6, 126.9, 126.7, 121.0, 31.2, 21.4.

2-Phenyl-5-(pyridin-4-yl)-1,3,4-oxadiazole.

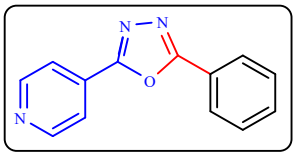

The general procedure was followed. Purification by recrystallization with EtOH gave the desired product as a white solid. M.p. 139–140 °C;[9] ^{1}H NMR (250 MHz, DMSO-d_6) δ 8.83 (s, 2H), 8.13 (d, J = 6.5 Hz, 2H), 8.03 (d, J = 5.0 Hz, 2H), 7.62 (d, J = 9.2 Hz, 3H). ^{13}C NMR (63 MHz, DMSO-d_6) δ 165.2, 162.9, 151.3, 132.8, 130.9, 129.9, 127.3, 123.4, 120.7. MS *m/z*: 223.2.

2-(4-Chlorophenyl)-5-(pyridin-4-yl)-1,3,4-oxadiazole

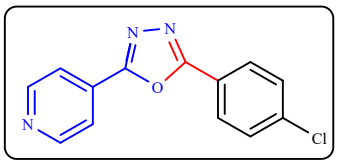

The general procedure was followed. Purification by recrystallization with EtOH gave the desired product as a white solid. M.p. 140–143 °C;[9] ^{1}H NMR (250 MHz, DMSO-d_6) δ 8.14 (d, J = 8.8 Hz, 4H), 7.70 (d, J = 7.5 Hz, 2H), 7.62 – 7.48 (d, J = 8 Hz, 2H), 2.42 (s, 3H). MS *m/z*: 257.04.

2-(Pyridin-4-yl)-5-(*p*-tolyl)-1,3,4-oxadiazole.

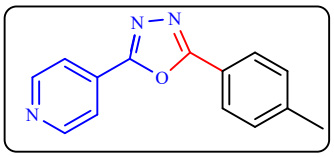

The general procedure was followed. Purification by recrystallization with EtOH gave the desired product as a white solid. M.p. 140–142 °C;[10] ^{1}H NMR (500 MHz, DMSO-d_6) δ 8.13 (d, J = 5 Hz, 2H), 8.04 – 8.00 (d, J = 2.5 Hz, 2H), 7.64 (d, J = 5 Hz, 2H), 7.44 (d, J = 7.9 Hz, 2H), 2.42 (s, 3H). ^{13}C NMR (125 MHz, dmso) δ 164.5, 164.2, 142.6, 132.4, 130.4, 130.4, 129.8, 127.1, 127.0, 123.8, 121.0, 21.6. MS *m/z*: 237.2.

2-(2-Chlorophenyl)-5-phenyl-1,3,4-oxadiazole

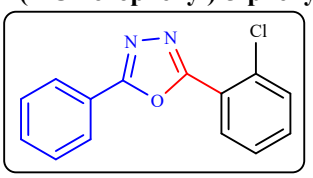

The general procedure was followed. Purification by column chromatography (silica gel, *n*-hexan/EtOAc, 10:3) gave the desired product as a yellow solid. M.p. 96–98 °C;[11] ^{1}H NMR (250 MHz, DMSO-d_6) δ 8.10 (ddt, J =

7.9, 4.6, 1.4 Hz, 3H), 7.73 (dt, *J* = 7.9, 1.3 Hz, 1H), 7.70 – 7.52 (m, 5H). ^{13}C NMR (125 MHz, DMSO-d_6) δ ^{13}C NMR (63 MHz, DMSO) δ 133.7, 132.7, 131.8, 131.6, 129.9, 128.3, 127.2, 123.5. MS *m/z*: 257.6.

4-(5-Phenyl-1,3,4-oxadiazol-2-yl) benzoic acid.

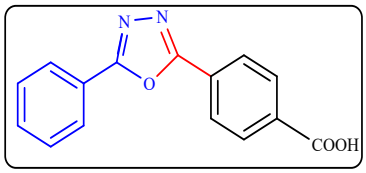

The general procedure was followed. Purification by recrystallization with EtOH gave the desired product as a yellow solid. M.p. 217–218°C,[12] ^{1}H NMR (500 MHz, DMSO-d_6) δ 12.6 (s, 1H), 8.34 (s, 1H), 8.24 (d, *J* = 8.0 Hz, 1H), 8.19 – 8.09 (m, 4H), 7.64 (d, *J* = 10Hz, 3H). ^{13}C NMR (126 MHz, DMSO-d_6) δ 166.9, 164.8, 163.9, 134.0, 132.6, 132.5, 130.6, 129.9, 129.8, 129.6, 128.0, 127.4, 127.3, 127.2, 127.1, 123.6. MS *m/z*: 266.6.

2-(4-Bromophenyl)-5-(3-methoxyphenyl)-1,3,4-oxadiazole.

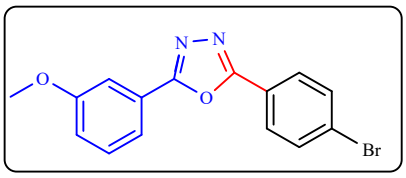

The general procedure was followed. Purification by recrystallization with EtOH gave the desired product as a white solid. M.p. 152–153 °C,[13] ^{1}H NMR (400 MHz, DMSO-d_6) δ 8.06 (d, *J* = 8.0 Hz, 2H), 7.82 (d, *J* = 8.0 Hz, 2H), 7.70 (d, *J* = 8.0 Hz, 1H), 7.60 (s, 1H), 7.54 (t, *J* = 7.7 Hz, 1H), 7.21 (dd, *J*= 8, 4 Hz, 1H), 3.89 (s, 3H). ^{13}C NMR (100 MHz, DMSO-d_6) δ 164.5, 164.4, 160.0, 132.6, 131.2, 129.8, 127.1, 124.6, 123.4, 119.4, 118.5, 111.9, 111.8, 55.8. MS *m/z*: 330.0.

2,5-Diphenyl-1,3,4-oxadiazole.

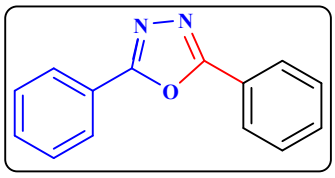

The general procedure was followed. Purification by recrystallization with EtOH gave the desired product as a white solid. M.p. 132–133 °C;[14] ^{1}H NMR (400 MHz, DMSO-d_6) δ 8.12 (dd, *J* = 8, 4 Hz,4H), 7.63 (m, 6H), ^{13}C NMR (101 MHz, DMSO) δ 164.6, 132.6, 129.9, 127.1, 123.5.

2-(4-Bromophenyl)-5-(p-tolyl)-1,3,4-oxadiazole.

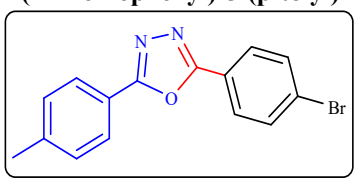

The general procedure was followed. Purification by recrystallization with EtOH gave the desired product as a white solid. M.p. 200–202 °C;[6] ^{1}H NMR (400 MHz, DMSO-d_6) δ 8.06 (d, *J* = 8.4 Hz,2H), 8.01 (d, *J* = 8 Hz,1H), 7.83 (d, *J* = 6 Hz, 2H), 7.65 (d, *J* = 8.4 Hz,1H), 7.44 (d, *J* = 8 Hz,2H), 2.49 (s, 3H). MS *m/z*: 315.0.

2-Phenyl-5-(*p*-tolyl)-1,3,4-oxadiazole.

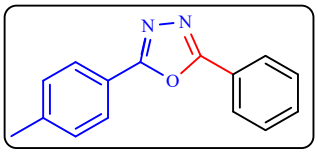

The general procedure was followed. Purification by recrystallization with EtOH gave the desired product as a white solid. M.p. 122–124°C;[14] ^{1}H NMR (400 MHz, DMSO-d_6) δ 8.13-8.10 (m, 3H), 8.06 (d, *J* = 9.6 Hz,1H), 7.82 (d, J = 8 Hz, 1H), 7.64 (t, *J* = 6.4 Hz, 4H), 2.51 (s, 3H). ^{13}C NMR (100 MHz, DMSO-d_6) δ 164.6, 163.8, 132.9, 132.0, 129.8, 129.0, 127.1, 126.1, 123.7, 123.0, 23.2. *m/z*: 236.

2-(3-Methoxyphenyl)-5-phenyl-1,3,4-oxadiazole.

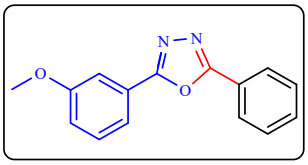

The general procedure was followed. Purification by recrystallization with EtOH gave the desired product as a white solid. M.p. 148-149°C;[1] ^{1}H NMR (400 MHz, DMSO-d_6) δ 8.09 (dd, 3.2, 1.2 Hz, 2H, 7.66 (dd, J = 7.7, 1.3 Hz, 1H), 7.64 – 7.59 (m, 3H), 7.56 (t, J = 1.6 Hz, 1H), 7.51 (t, J = 8.0 Hz, 1H), 7.21 (dd, 4.0, 2.8 Hz, 1H), 3.82 (s, 3H). ^{13}C NMR (100 MHz, DMSO-d_6) δ 164.5, 164.4, 160.0, 132.6, 131.2, 129.8, 127.1, 124.6, 123.4, 119.4, 118.5, 111.9, 111.8, 55.8. *m/z*: 252.2.

2-(4-Bromophenyl)-5-(pyridin-4-yl)-1,3,4-oxadiazole.

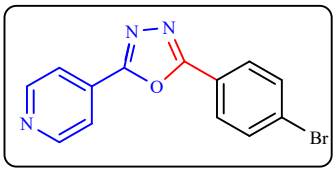

The general procedure was followed. Purification by recrystallization with EtOH gave the desired product as a white solid. M.p. 180°C,[15] ^{1}H NMR (400 MHz, DMSO-d_6) δ 8.83 (d, J = 5.8 Hz, 2H), 8.08 (dd, J = 10.0, 7.3 Hz, 4H), 7.84 (d, J = 8.5 Hz, 2H). ^{13}C NMR (101 MHz, DMSO-d_6) δ 151.2, 133.0, 129.3, 120.9. *m/z*: 300.1.

2-(2,3-Dichlorophenyl)-5-phenyl-1,3,4-oxadiazole.

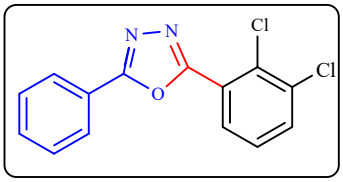

The general procedure was followed. Purification by column chromatography (silica gel, *n*-hexan/EtOAc, 10:3) gave the desired product as a yellow solid. M.p. 146–147 °C; ^{1}H NMR (400 MHz, DMSO-d_6) δ 8.51 (ddd, J = 7.8, 6.7, 1.4 Hz, 2H), 8.29 (t, J = 7.9 Hz, 2H), 7.96 (t, J = 7.8 Hz, 2H), 7.57 (dd, J = 2, 1.2 *Hz*, 2H), 7.49 (t, J= 7.6 Hz, 1H). ^{13}C NMR (100 MHz, DMSO) δ 155.5, 134.6, 132.6, 131.2, 129.1, 128.7, 127.9, 118.6, 118.5, 118.3.

2-(2-Methoxyphenyl)-5-phenyl-1,3,4-oxadiazole.

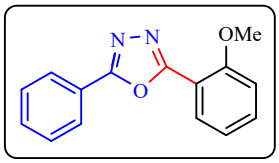

The general procedure was followed. Purification by column chromatography (silica gel, *n*-hexan/EtOAc, 10:3) gave the desired product as a yellow solid. M.p. 118-120 °C;[1] ^{1}H NMR (400 MHz, DMSO-d_6) δ 7.60 (d, J = 6.4 Hz, 2H), 7.44 (t, J = 7.8 Hz, 2H), 7.20 (t, J = 7.8 Hz, 2H), 7.13 (d, J = 8.3 Hz, 1H), 7.07 (t, J = 7.5 Hz, 1H), 6.74 (t, J = 7.3 Hz, 1H), 3.87 (s, 3H). ^{13}C NMR (101 MHz, DMSO) δ 156.4, 145.9, 130.5, 129.0, 128.4, 120.6, 119.3, 118.1, 113.6, 113.6, 111.5, 55.7.

2-(4-Fluorophenyl)-5-phenyl-1,3,4-oxadiazole.

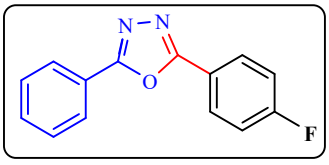

The general procedure was followed. Purification by recrystallization with EtOH gave the desired product as a yellow solid, M.p. 150-151 °C;[14]^{1}H NMR (400 MHz, DMSO-d_6) δ 8.64 (t, J =5.6 Hz, 2H), 8.33 (t, J = 8.7 Hz, 2H), 8.19 (t, J = 7.7 Hz, 2H), 7.84 (d, J = 7.9 Hz, 1H), 7.75 (t, J = 7.3 Hz, 1H), 7.70 (d, J = 9.6 Hz, 1H). ^{13}C NMR (101 MHz, DMSO-d_6) δ 163.3, 160.9, 145.7, 129.0, 119.4, 116.4, 115.9, 115.6, 113.8.

2-(4-Methoxyphenyl)-5-phenyl-1,3,4-oxadiazole.

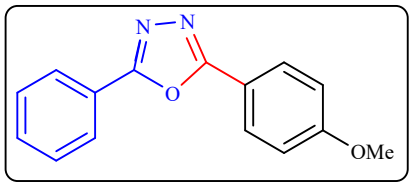

Known compound, the general procedure was followed. Purification by recrystallization with EtOH gave the desired product as a white solid; M.p. 149-150 °C.[14]

2-(4-Chlorophenyl)-5-phenyl-1,3,4-oxadiazole:

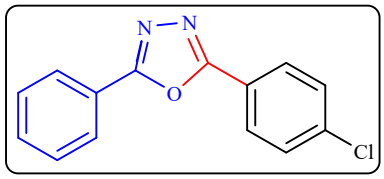

Known compound, the general procedure was followed. Purification by recrystallization with EtOH gave the desired product as a white solid; M.p. 159-160 °C.[14]

References:

1. Li. Zhengyi, W. Liang, *Adv. Synth. Catal*. 2015, **357**, 3469 – 3473.
2. S. J. Gilani, S. Ahmad Khan and N. Siddiqui, Acta Poloniae Pharmaceutica-Drug Research, 2011, **68**, 205-211.
3. Y. Fanzhi, K. Julian, A. Lutz, *Angew. Chem*. 2016, **128**, 4837 – 4840.
4. R. Chandra Sekhar, *Synth. Commun*. 2004, **34**, 2153 – 2157.
5. L. Qiang, T. Yi, X. Dongfang, Z. Haobing, D. Liping, *J. Chin. Chem. Soc.* 2014, **61**, 665 – 670.
6. G. Peng, W. Yunyang, *Heterocycl Comm*, 2013, **19**, 113 – 119.
7. W. Kun-Li; L. Gang, C. Po-Hao, P. Liang, T. Hsin-Luen, *Org. Electron*. 2014, **15**, 322 – 336.
8. M. Tomoya, H. Koji, S.Tetsuya, M. Masahiro, *Org. Lett*. 2010, **12**, 1360 – 1363.
9. M. Geeta Sai, D. Kavitha, S. Nagula, K. Ahmed, *New. J. Chem*. 2019, **43**, 15999 – 16006.
10. Y. Wenquan, H. Gang, Z. Yueteng, L. Hongxu, D. Lihong, Y. Xuejun, L. Yujiang, C. Junbiao, *J. Org. Chem*. 2013, **78**, 10337 – 10343.
11. W. Liang, C. Jing, C. Qun, He. Mingyang, *J. Org. Chem*. 2015, **80**, 4743 – 4748.
12. A.P. Grekow, O.P. Schvaika, Journal of general chemistry of the USSR, 1960, **30**, 3763 – 3766.
13. S. Zhenhua, *Synth. Commun*. 2006, **36**, 2927 – 2937.
14. G. Majji, S. Kumar Rout, S. Guin, A. Gogoi and B. K. Patel, *RSC Adv*. 2014, **4**, 5357
15. P. Parikh, *J. Indian. Chem. Soc*. 1989, **66**, 250 – 251.

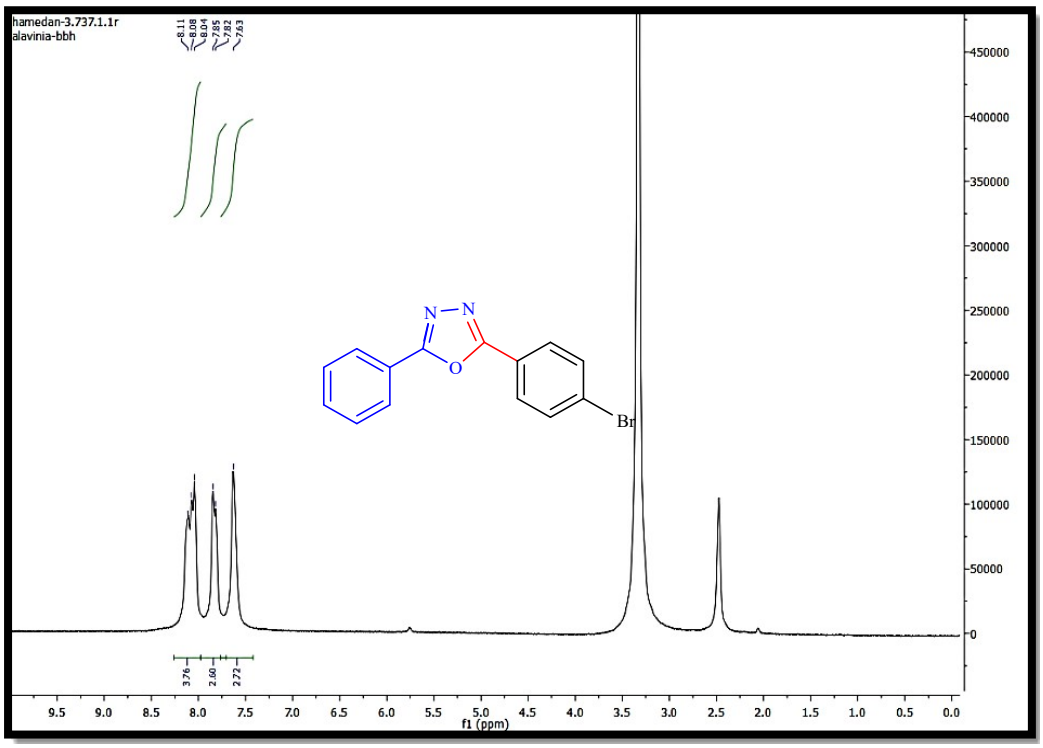
hamedan-3.737.1.1r
alavinia-bbh
8.11
8.08
8.04
7.85
7.82
7.83
N
N
O
Br
3.76
2.00
2.72
450000
400000
350000
300000
250000
200000
150000
100000
50000
0
9.5
9.0
8.5
8.0
7.5
7.0
6.5
6.0
5.5
5.0
4.5
4.0
3.5
3.0
2.5
2.0
1.5
1.0
0.5
0.0
f1 (ppm)

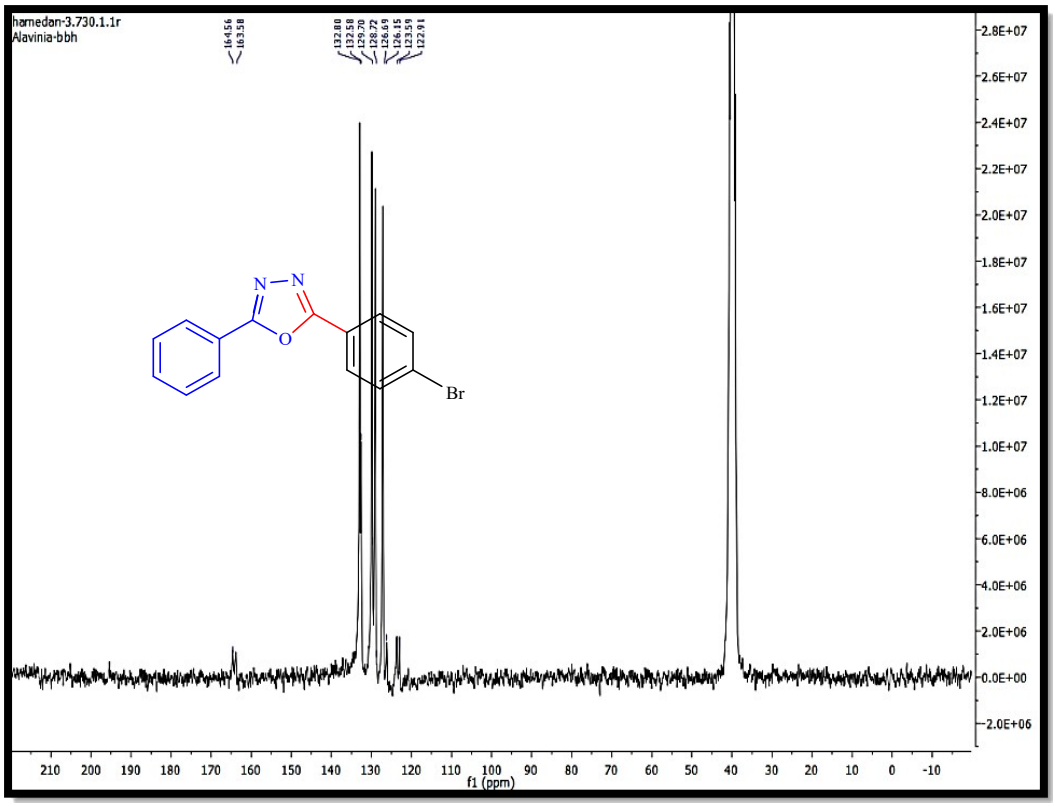
harnedan-3.730.1.1r
Alavinia-bbh
164.56
163.58
132.80
131.58
129.70
128.72
126.69
126.15
123.59
122.91
N
N
O
Br
f1 (ppm)

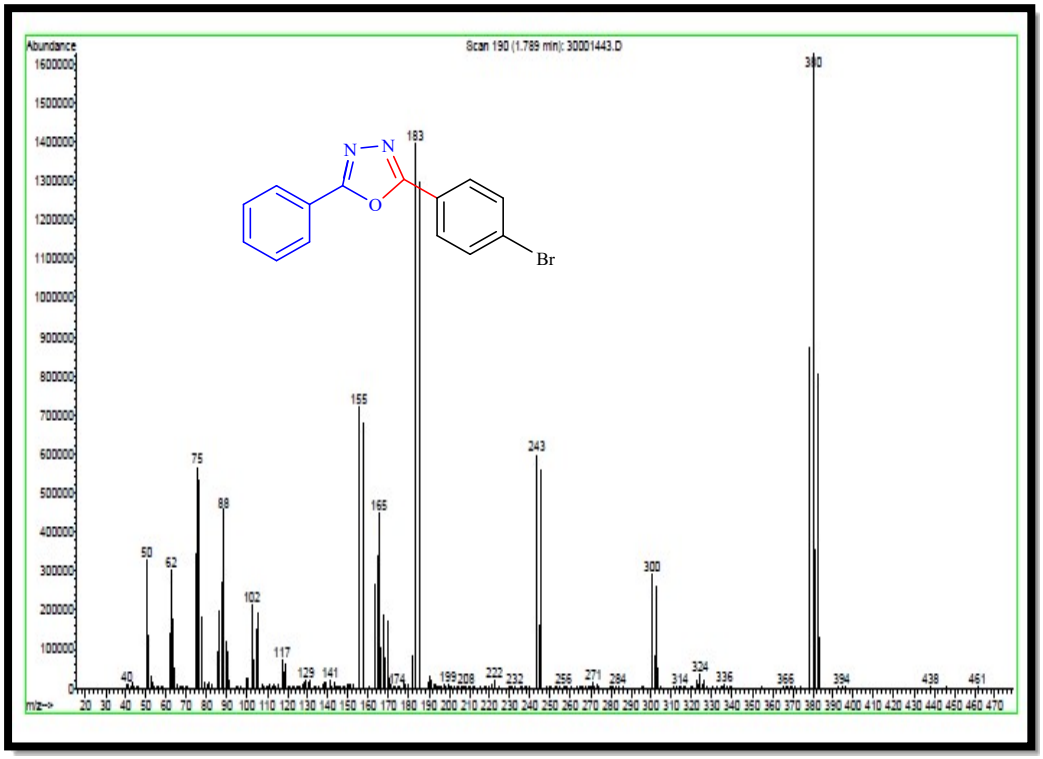
Abundance
Scan 190 (1.789 min): 30001443.D
N
N
O
Br
m/z->

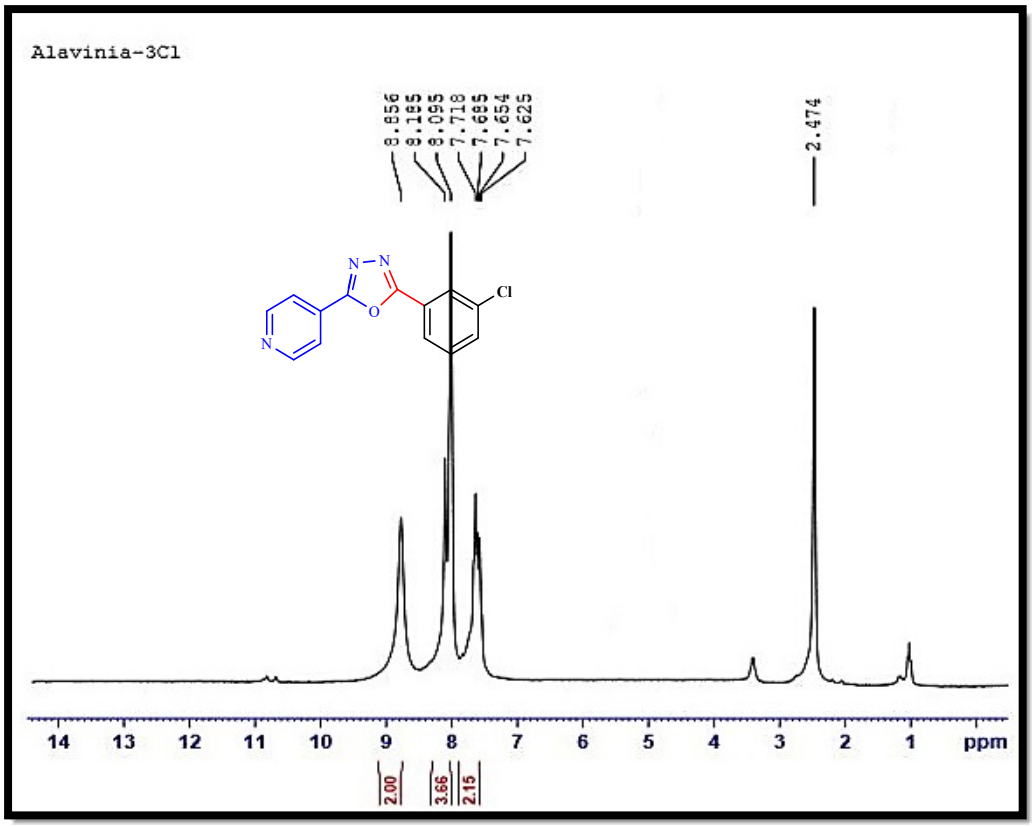
Alavinia-3Cl
8.856
8.185
8.095
7.718
7.685
7.654
7.625
2.474
Cl
N
N
O
N
14
13
12
11
10
9
8
7
6
5
4
3
2
1
ppm
2.00
3.66
2.15

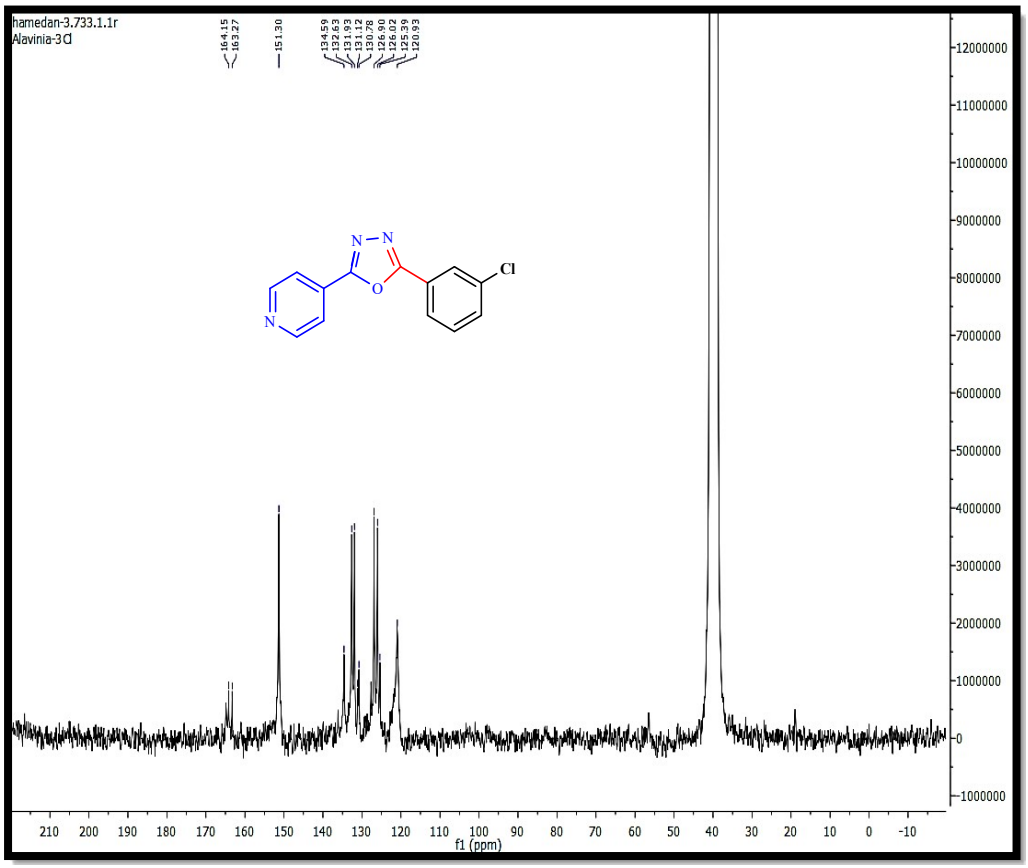
hamedan-3.733.1.1r
Alavinia-3Cl
164.15
163.27
151.30
134.59
132.58
131.93
131.12
130.78
126.90
126.72
125.98
120.93
Cl
N
N
O
N
12000000
11000000
10000000
9000000
8000000
7000000
6000000
5000000
4000000
3000000
2000000
1000000
0
-1000000
210
200
190
180
170
160
150
140
130
120
110
100
90
80
70
60
50
40
30
20
10
0
-10
f1 (ppm)

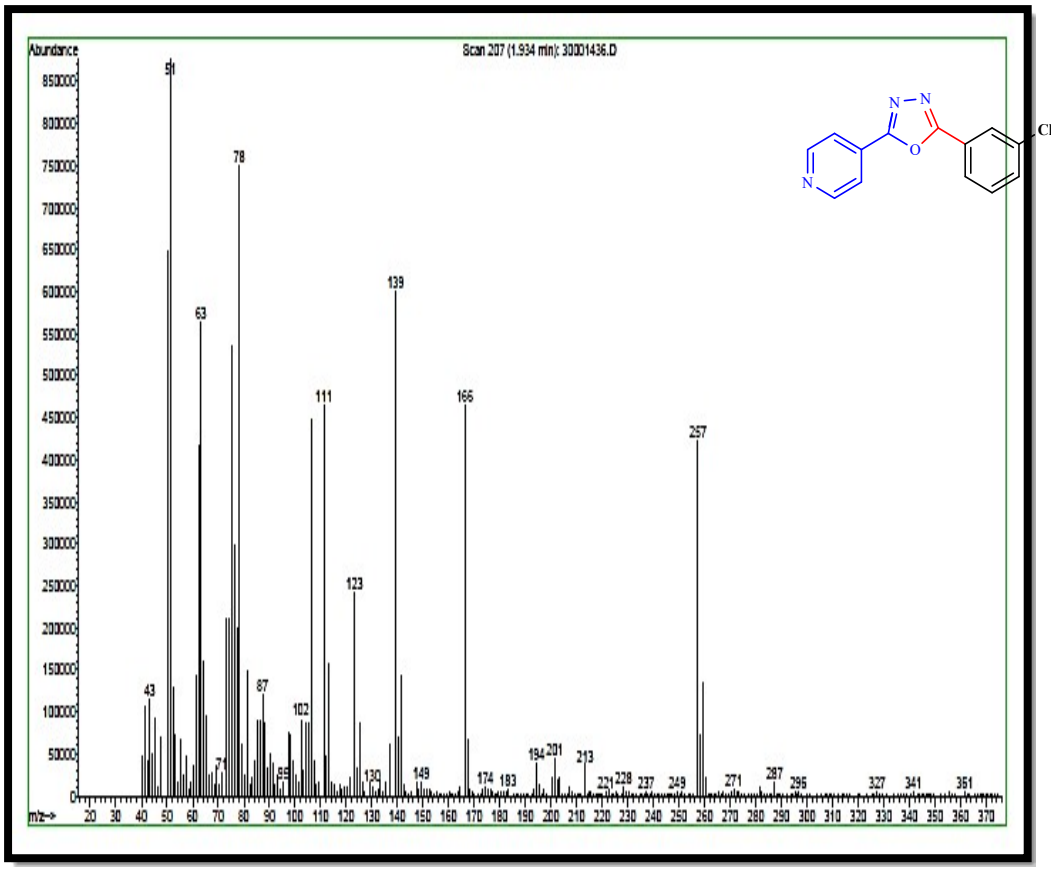
Abundance
Scan 207 (1.934 min): 30001436.D
m/z-->
Cl

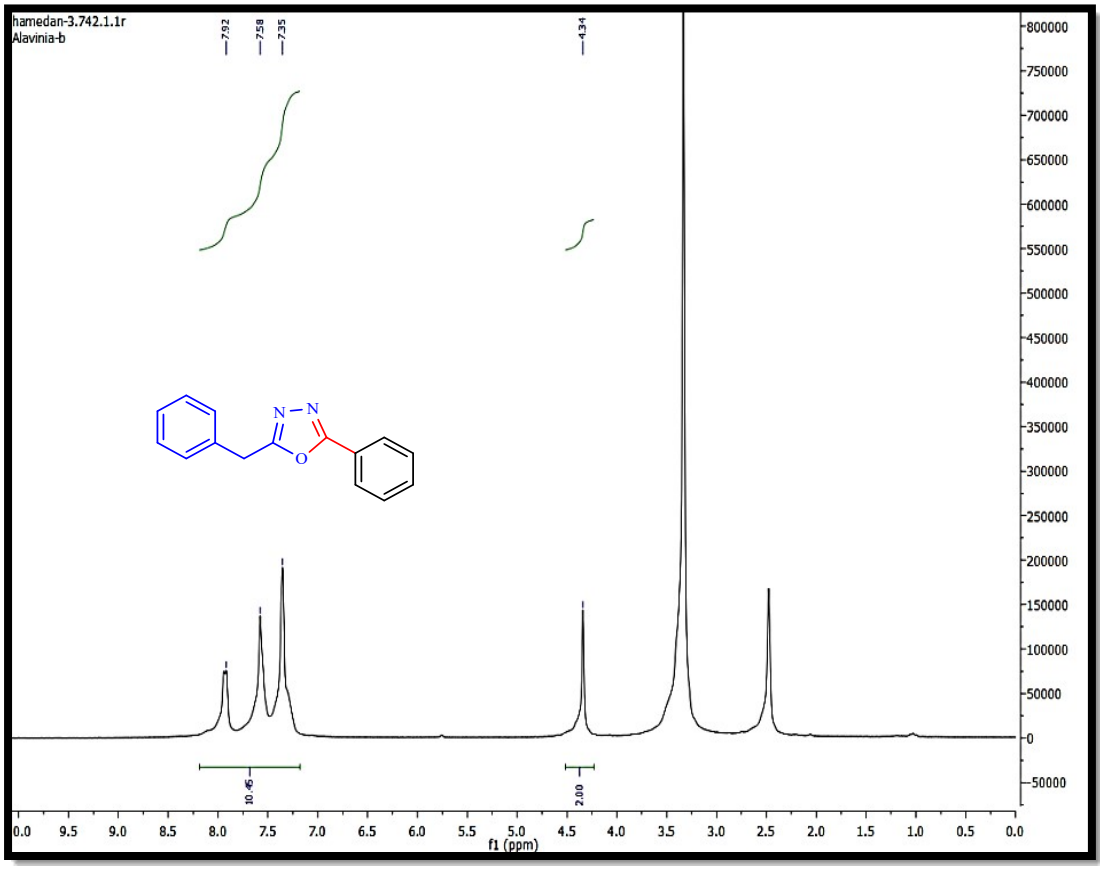
hamedan-3.742.1.1r
Alavinia-b
7.92
7.58
7.35
4.34
10.45
2.00
f1 (ppm)

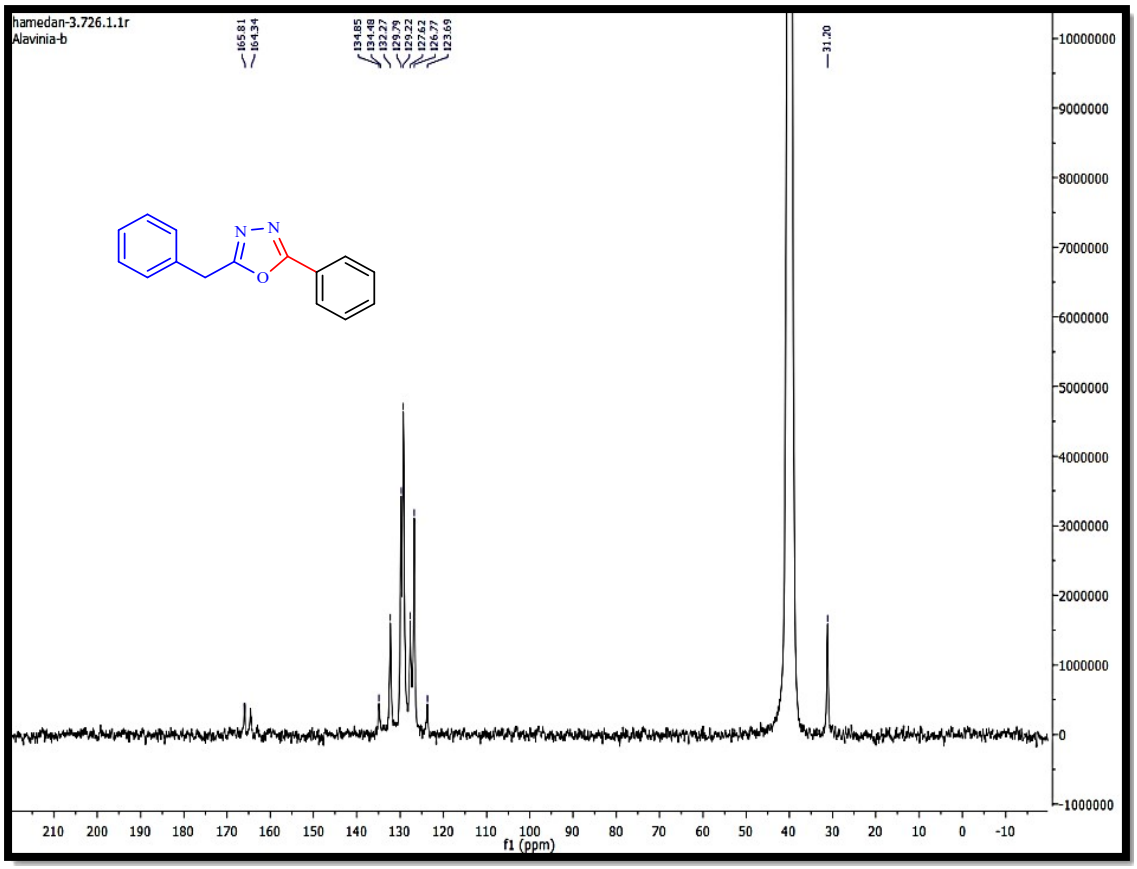
hamedan-3.726.1.1r
Alavinia-b
165.81
164.34
134.85
134.48
132.27
129.79
129.22
127.62
126.77
123.69
31.20
f1 (ppm)

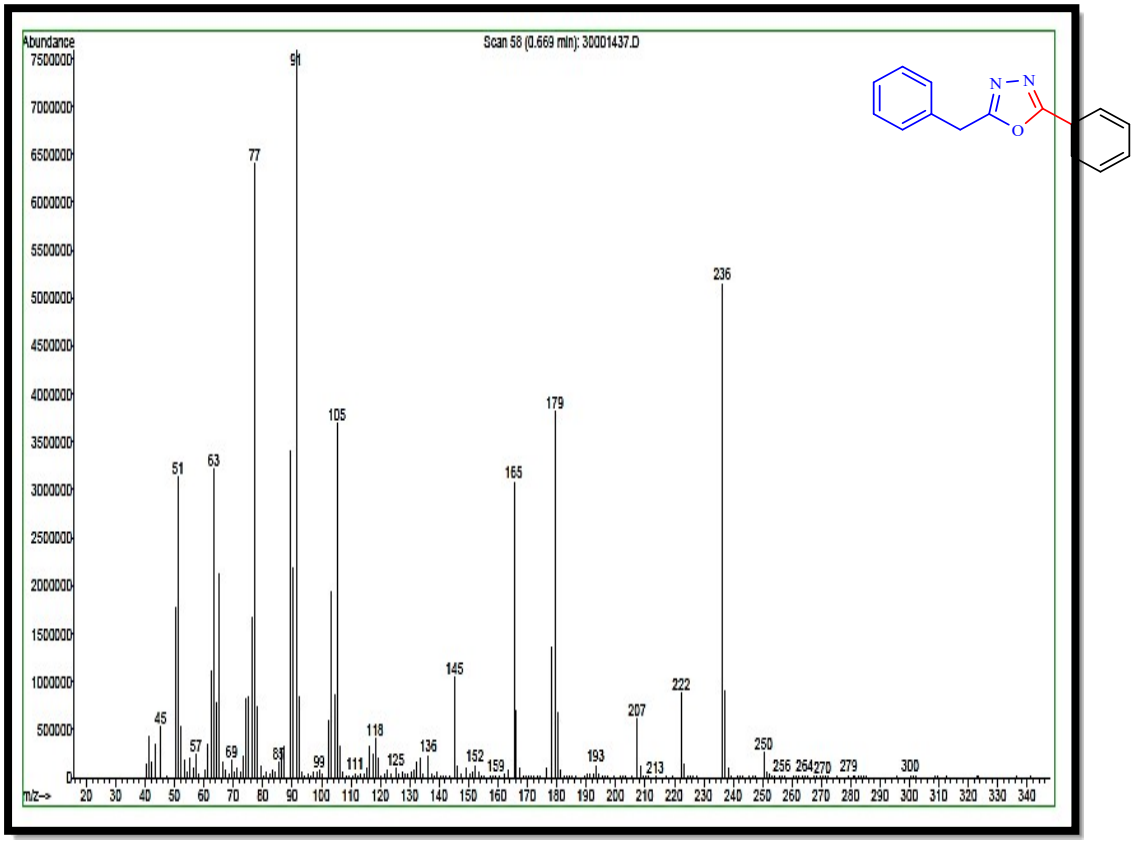
Abundance
Scan 58 (0.669 min): 30001437.D
m/z-->

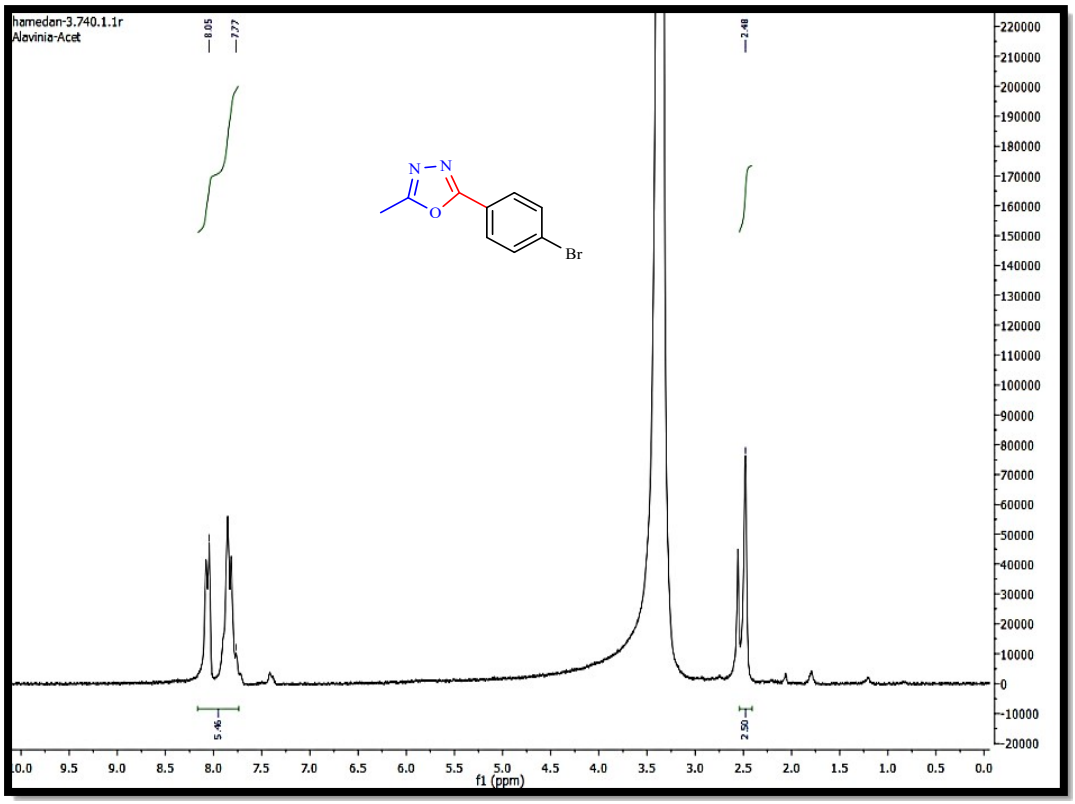
hamedan-3.740.1.1r
Alavinia-Acet
8.05
7.77
2.48
5.46
2.50
f1 (ppm)
Br

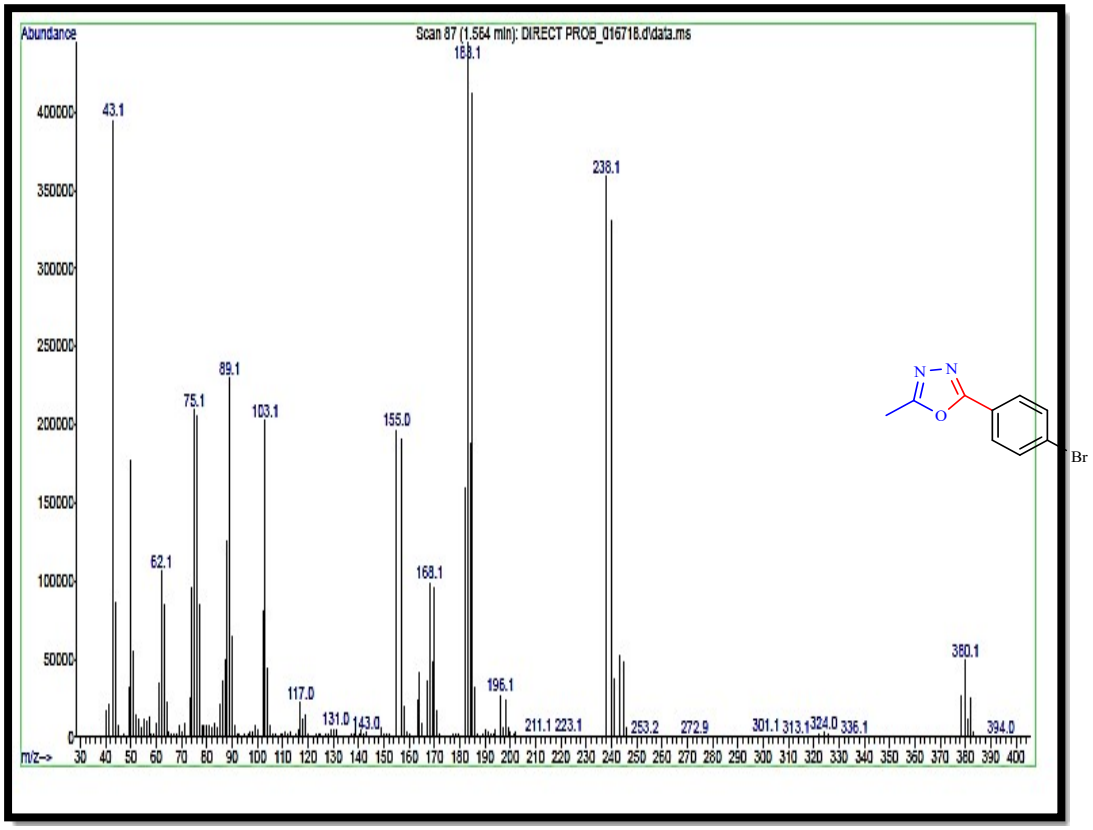
Abundance
Scan 87 (1.564 min): DIRECT PROB_016718.d\data.ms
m/z-->
Br

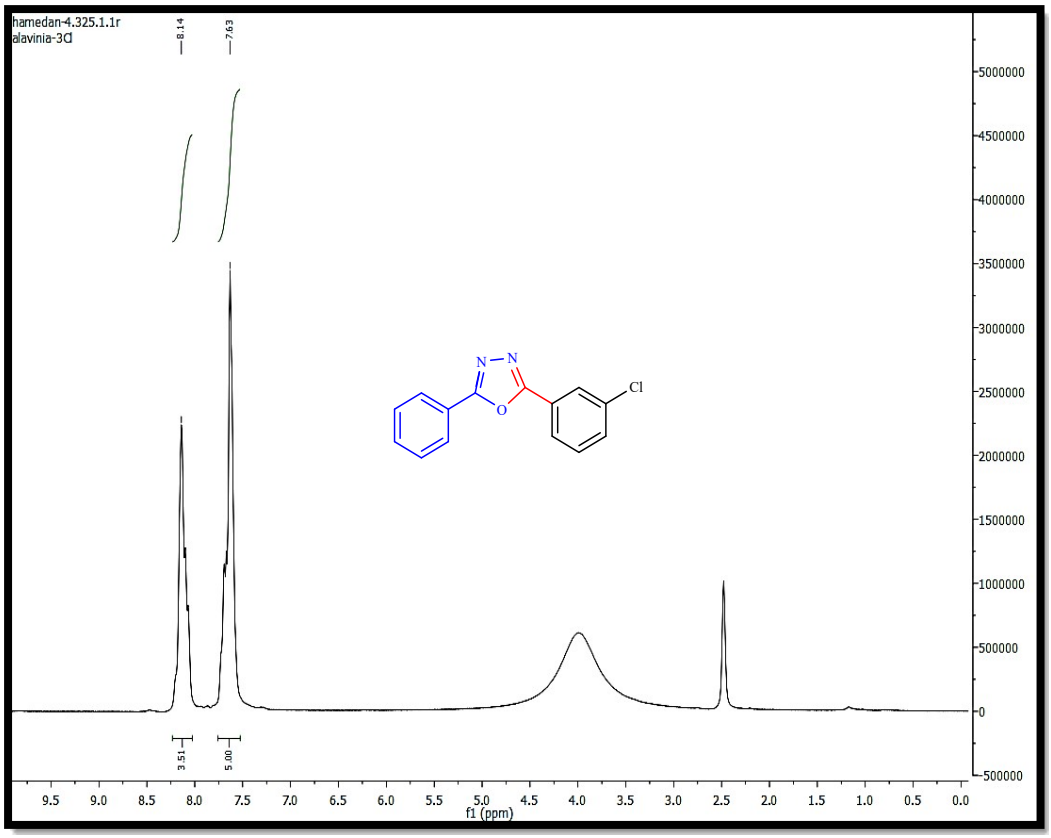
hamedan-4.325.1.1r
alavinia-3Cl
8.14
7.63
3.51
5.00
f1 (ppm)
N
N
O
Cl

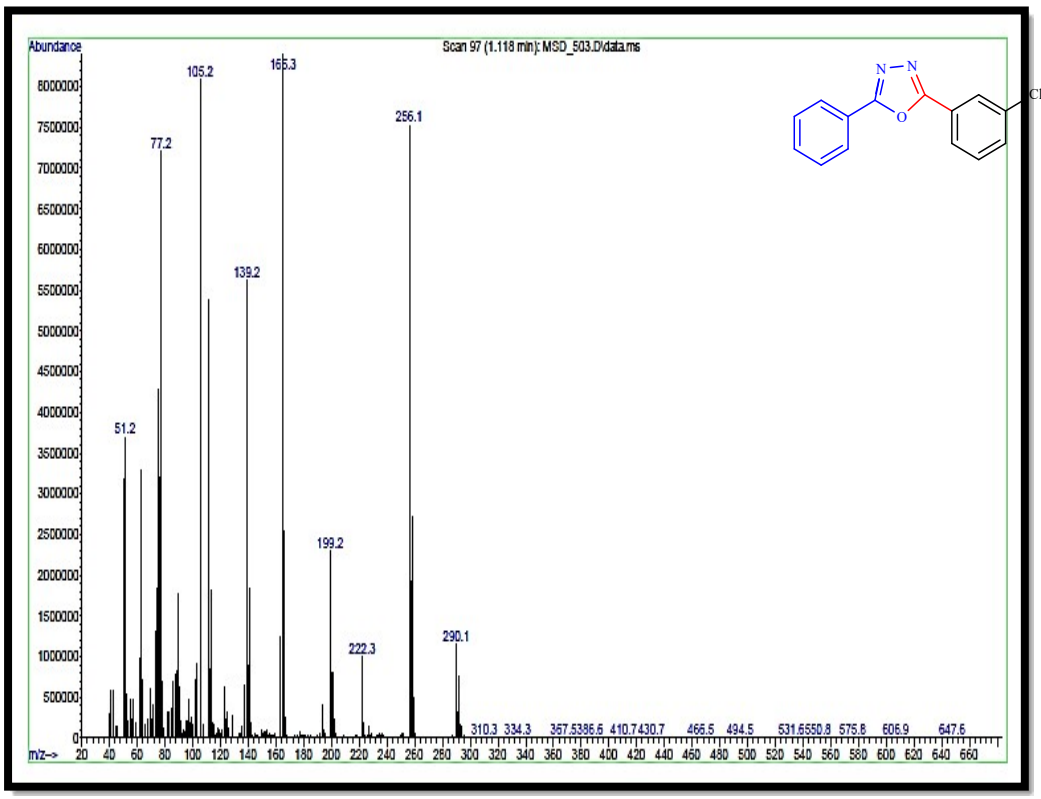
Abundance
Scan 97 (1.118 min): MSD_503.D\data.ms
105.2
165.3
256.1
77.2
139.2
51.2
199.2
222.3
290.1
m/z-->
N
N
O
Cl

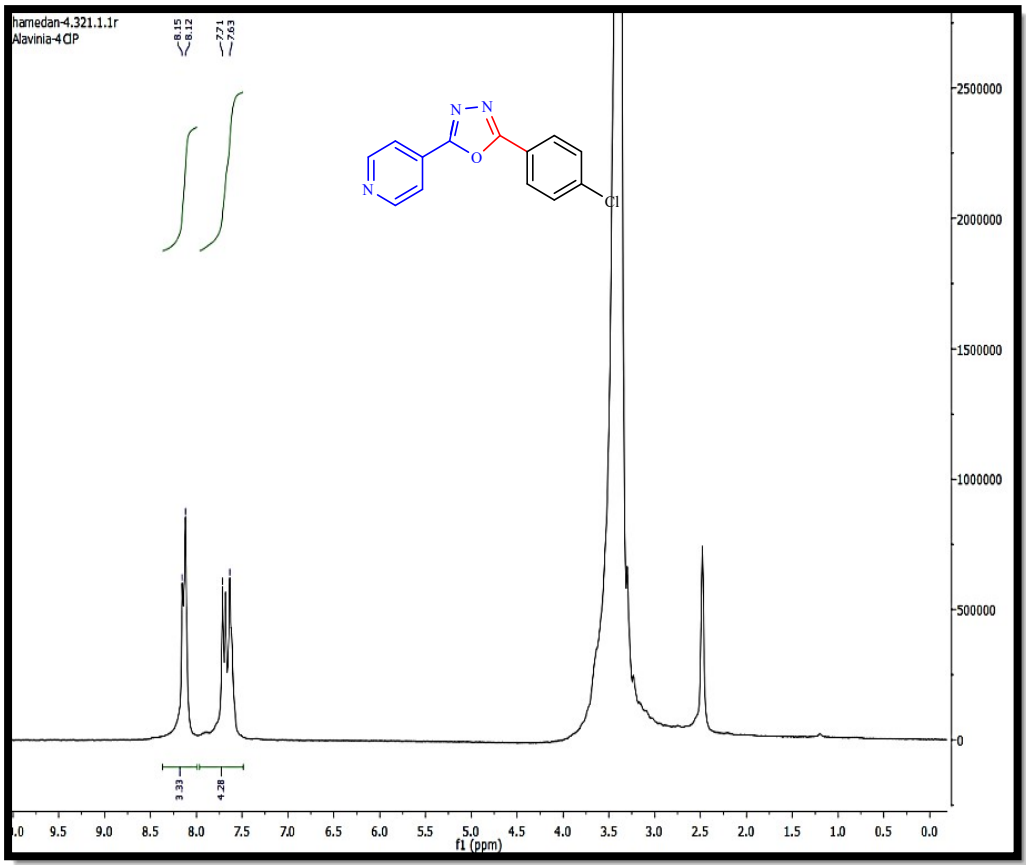
hamedan-4.321.1.1r
Alavinia-4 CP
8.15
8.12
7.71
7.63
N
N
O
N
Cl
2500000
2000000
1500000
1000000
500000
0
3.33
4.28
f1 (ppm)

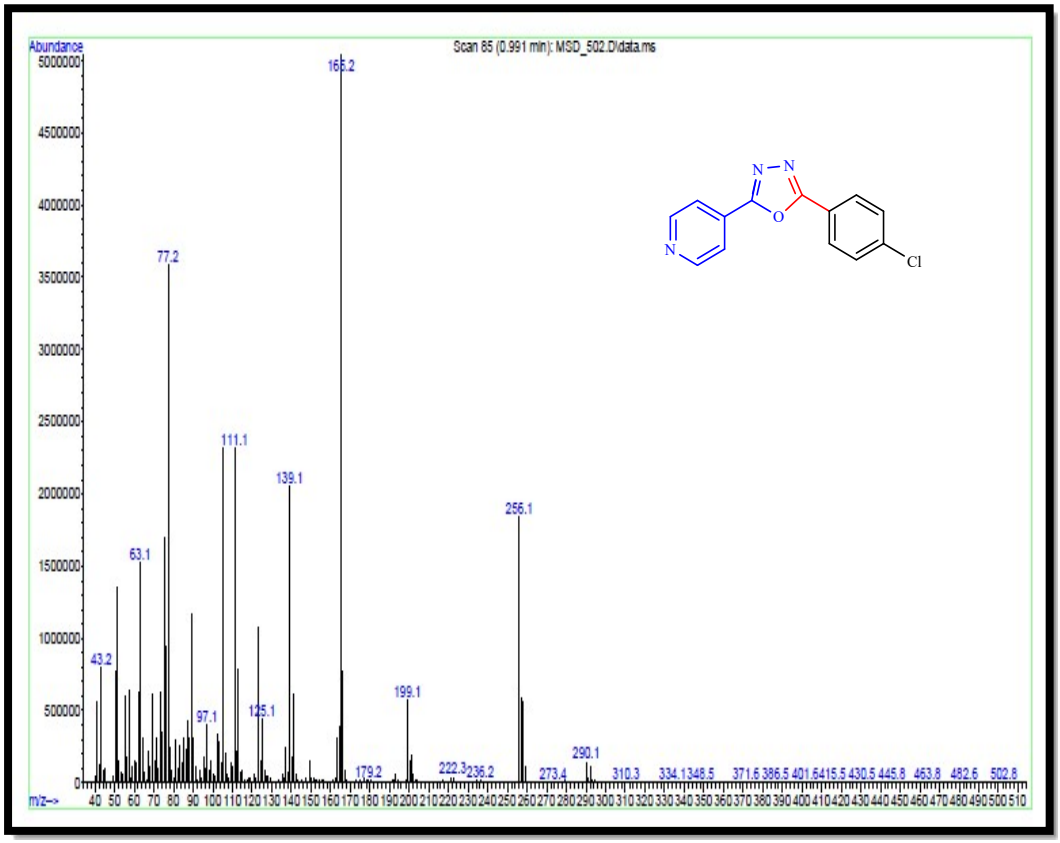
Abundance
Scan 85 (0.991 min): MSD_502.D\data.ms
166.2
77.2
111.1
139.1
256.1
63.1
43.2
199.1
97.1
125.1
290.1
179.2
222.3
236.2
273.4
310.3
334.1
348.5
371.6
386.5
401.6
415.5
430.5
445.8
463.8
482.6
502.8
m/z-->
N
N
O
N
Cl

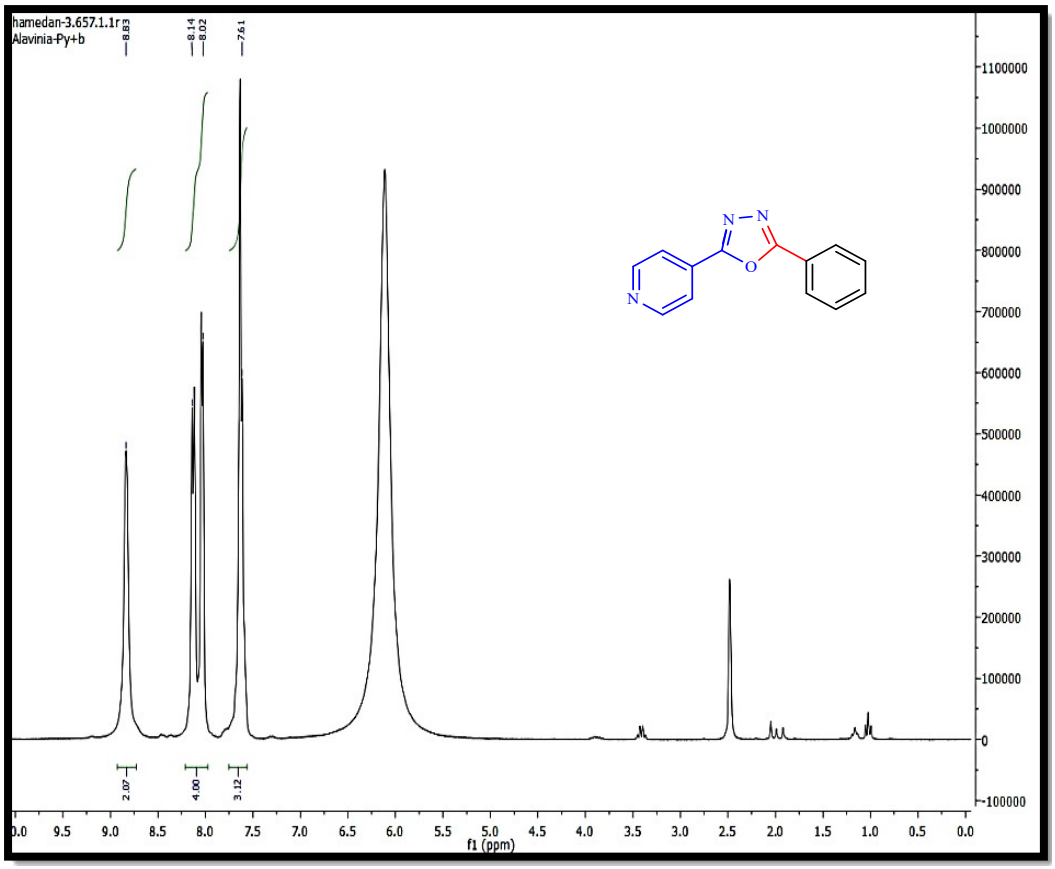
hamedan-3.657.1.1r
Alavinia-Py+b
8.83
8.14
8.02
7.61
2.07
4.00
3.12
f1 (ppm)

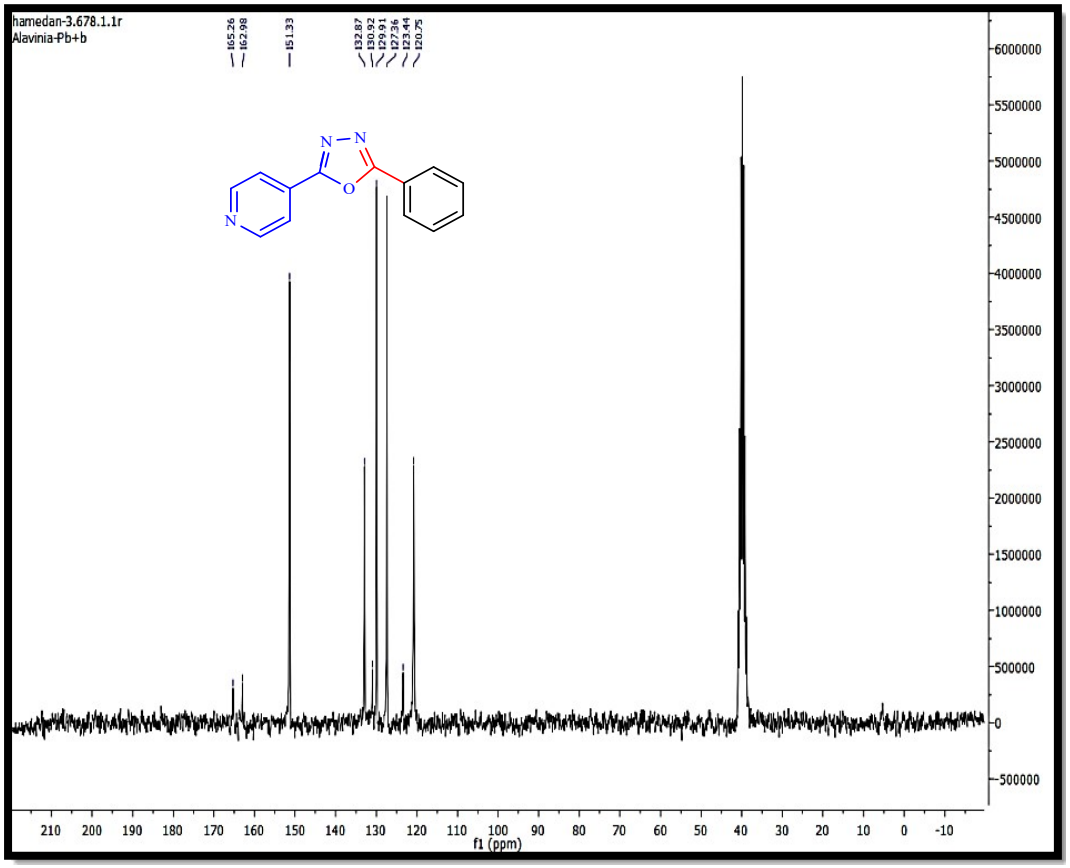
hamedan-3.678.1.1r
Alavinia-Pb+b
165.26
162.98
151.33
132.87
130.92
129.91
127.36
123.44
120.75
f1 (ppm)

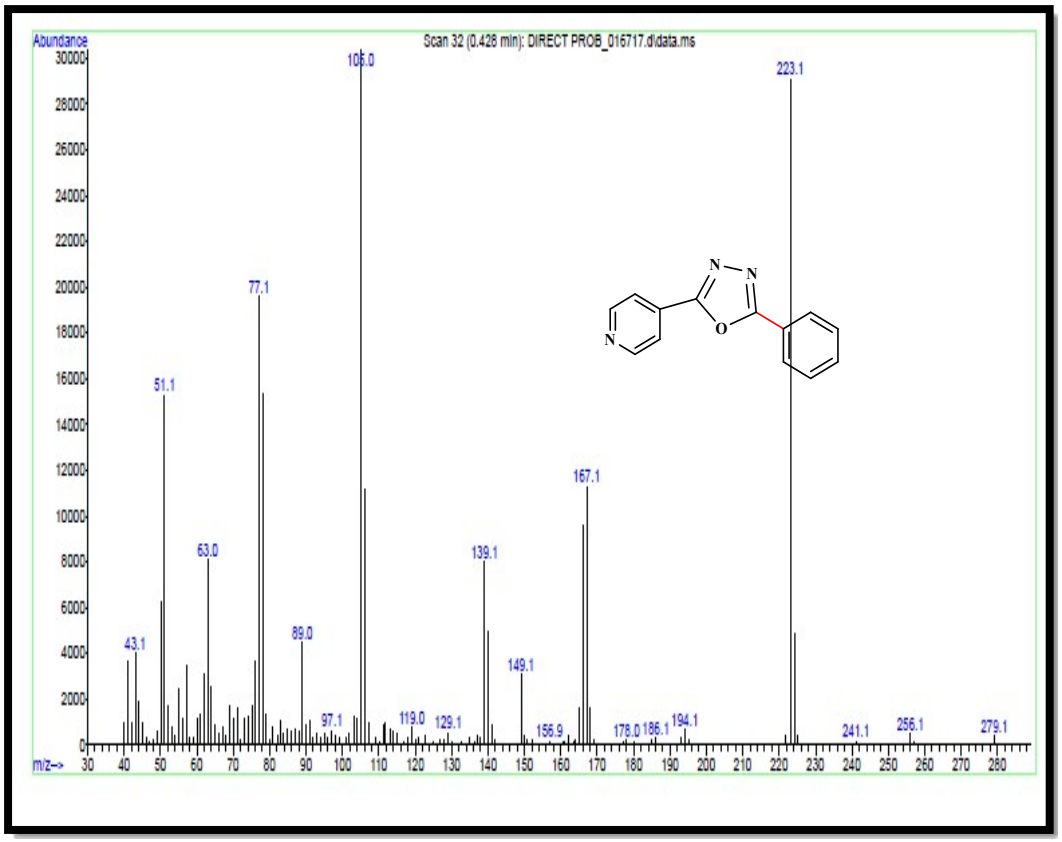
Abundance
Scan 32 (0.428 min): DIRECT PROB_016717.d\data.ms
106.0
223.1
77.1
51.1
167.1
63.0
139.1
89.0
43.1
149.1
97.1
119.0
129.1
156.9
176.0
186.1
194.1
241.1
256.1
279.1
m/z-->

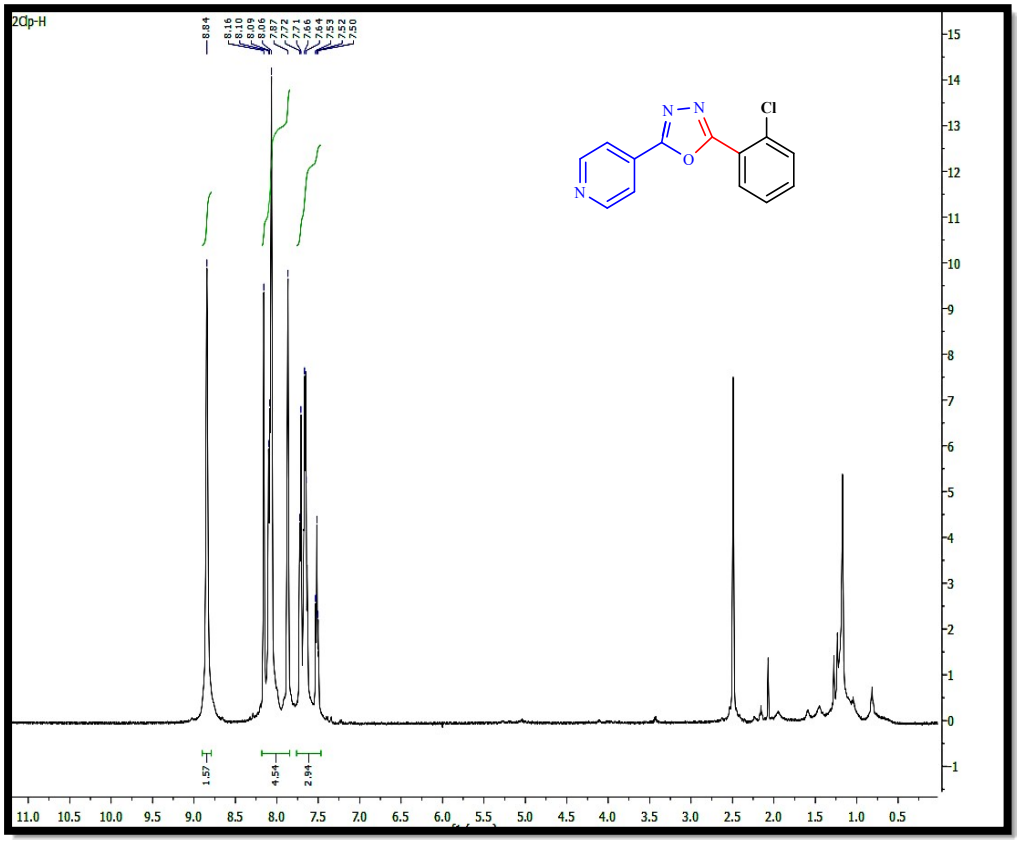
2Clp-H
8.84
8.16
8.10
8.09
8.06
7.87
7.72
7.71
7.66
7.64
7.53
7.52
7.50
Cl
1.57
4.54
2.94

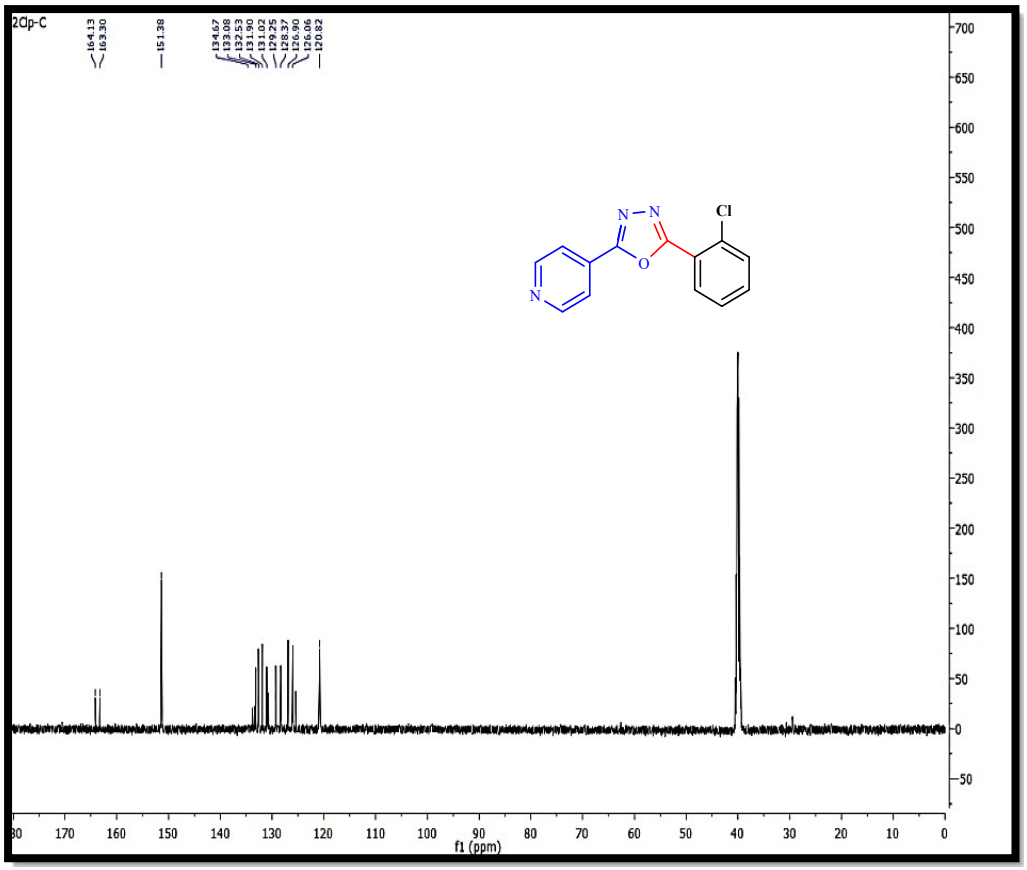
2Clp-C
164.13
163.30
151.38
134.67
133.08
132.53
131.56
131.02
129.25
128.37
126.90
126.66
120.82
Cl
N
N
O
N
f1 (ppm)

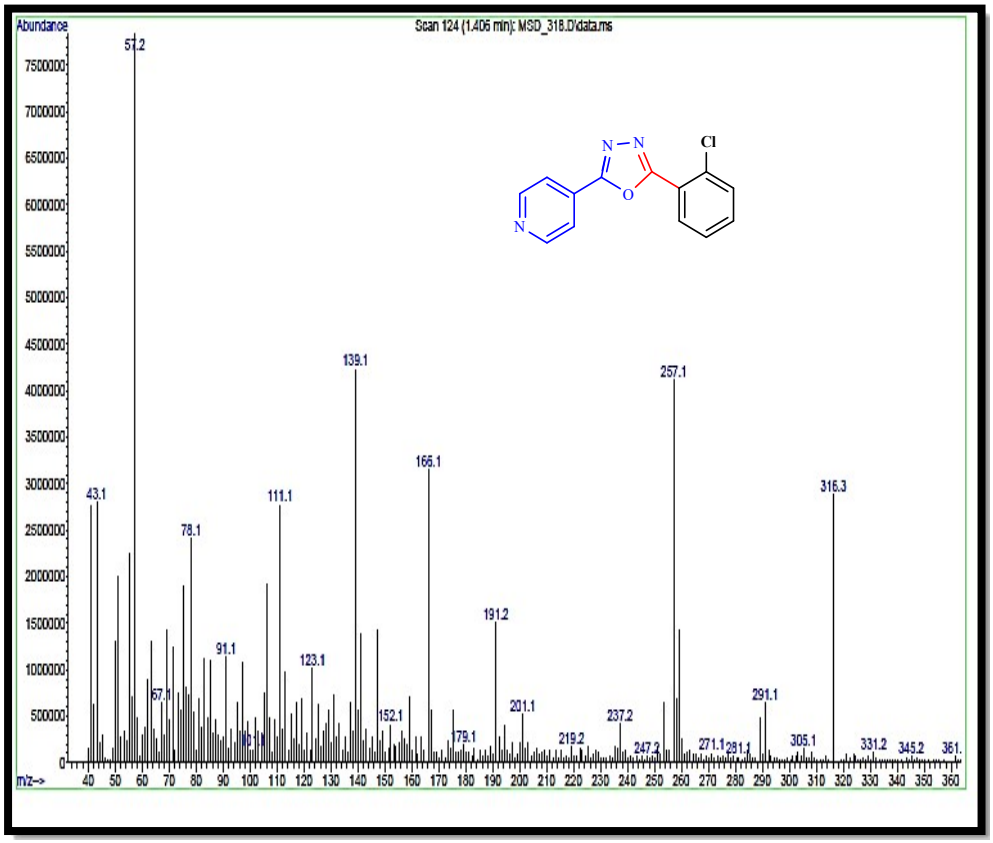
Abundance
Scan 124 (1.405 min): MSD_318.D\data.ms
57.2
139.1
257.1
166.1
316.3
43.1
111.1
78.1
191.2
91.1
123.1
67.1
201.1
237.2
291.1
152.1
179.1
219.2
247.2
271.1
281.1
305.1
331.2
345.2
361.
Cl
N
N
O
N
m/z-->

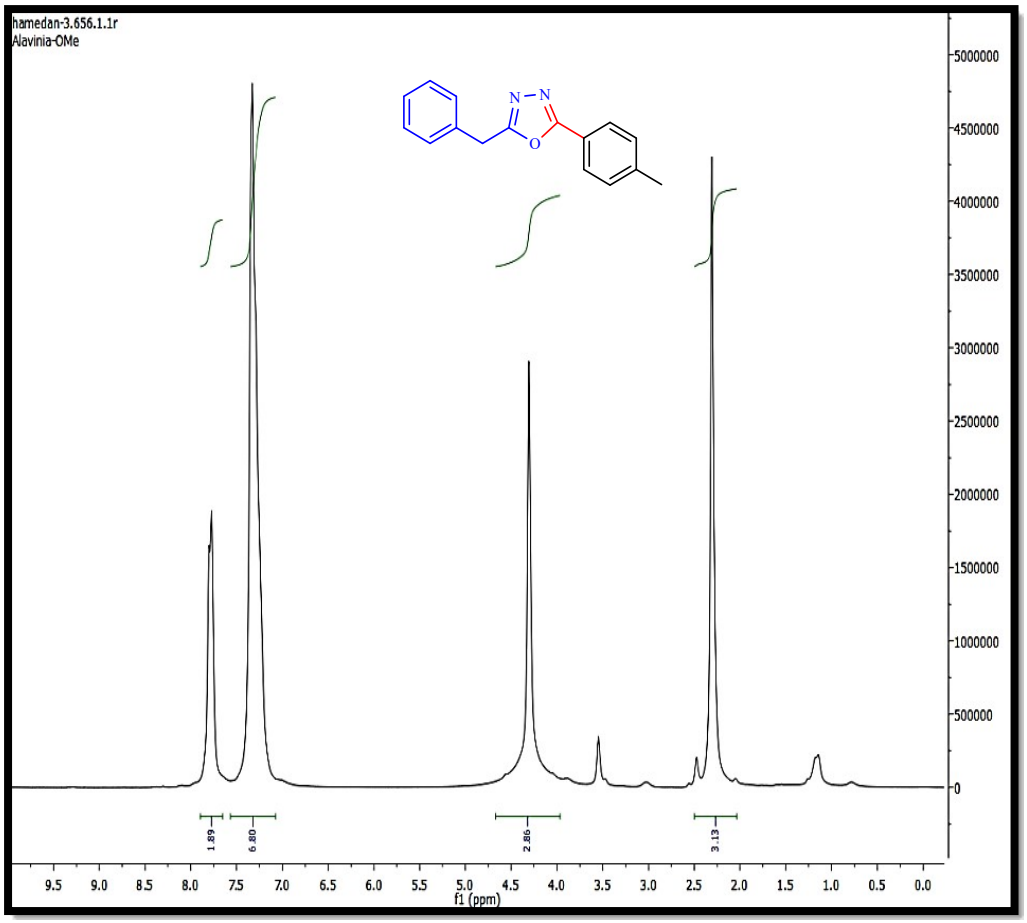
hamedan-3.656.1.1r
Alavinia-OMe
N
N
O
5000000
4500000
4000000
3500000
3000000
2500000
2000000
1500000
1000000
500000
0
1.89
6.80
2.86
3.13
9.5 9.0 8.5 8.0 7.5 7.0 6.5 6.0 5.5 5.0 4.5 4.0 3.5 3.0 2.5 2.0 1.5 1.0 0.5 0.0
f1 (ppm)

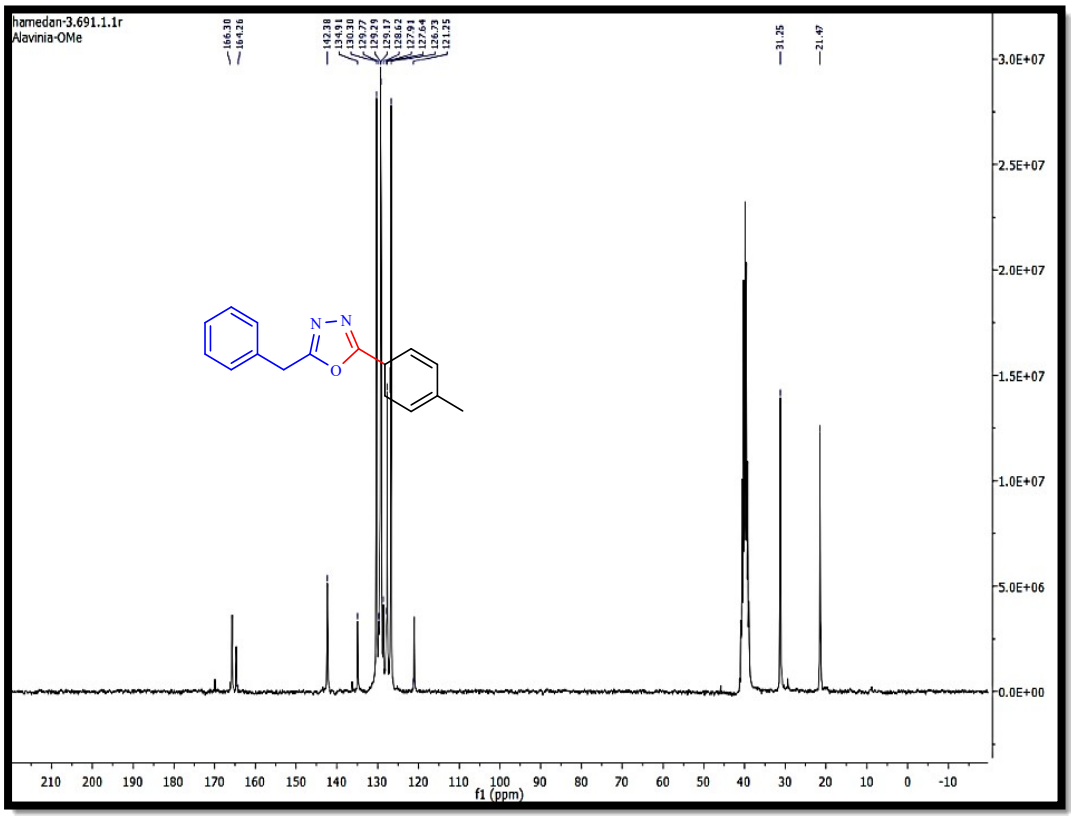
hamedan-3.691.1.1r
Alavinia-OMe
166.30
164.26
142.38
134.91
130.30
130.27
129.29
129.17
128.62
127.91
127.64
126.73
121.25
31.25
21.47
N
N
O
3.0E+07
2.5E+07
2.0E+07
1.5E+07
1.0E+07
5.0E+06
0.0E+00
210 200 190 180 170 160 150 140 130 120 110 100 90 80 70 60 50 40 30 20 10 0 -10
f1 (ppm)

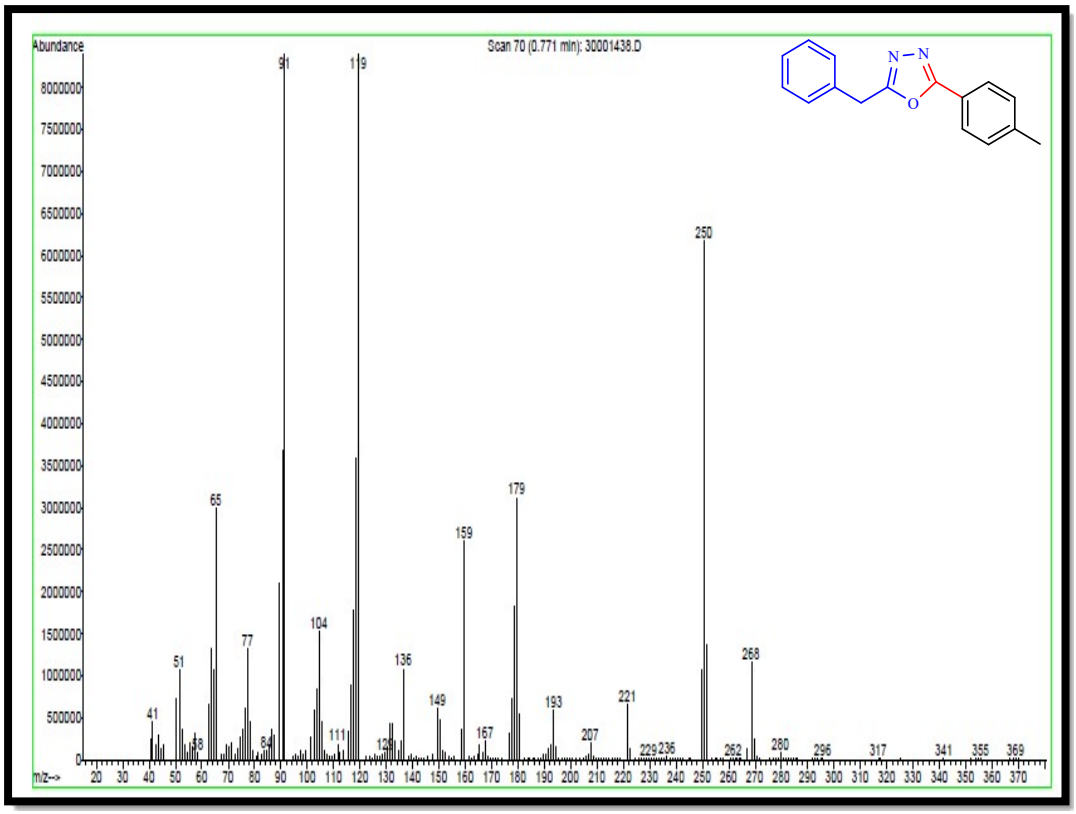
Abundance
Scan 70 (0.771 min): 30001438.D
m/z-->
91
119
250
65
179
159
104
77
136
51
149
193
221
268
41
167
207
280
296
317
341
355
369

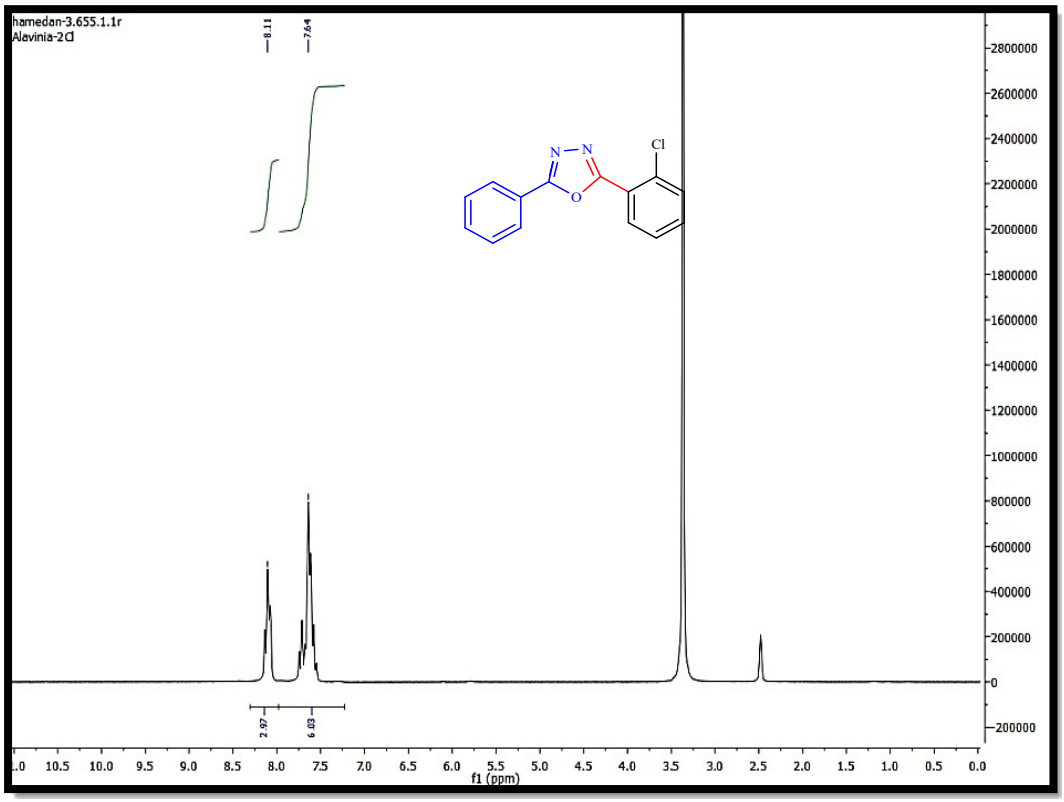
hamedan-3.655.1.1r
Alavinia-2Cl
0.11
7.64
Cl
2.97
6.03
f1 (ppm)

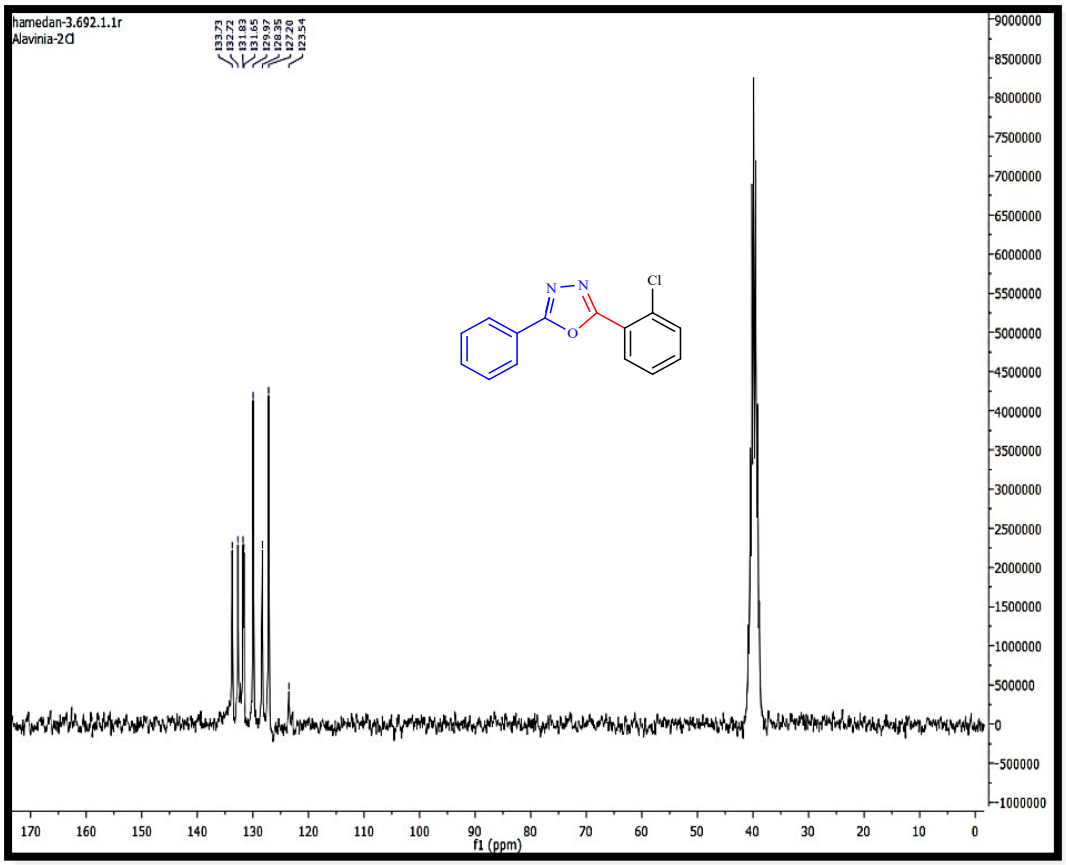
hamedan-3.692.1.1r
Alavinia-2Cl
133.73
132.72
131.83
131.65
129.37
128.35
127.20
123.54
N
N
O
Cl
f1 (ppm)

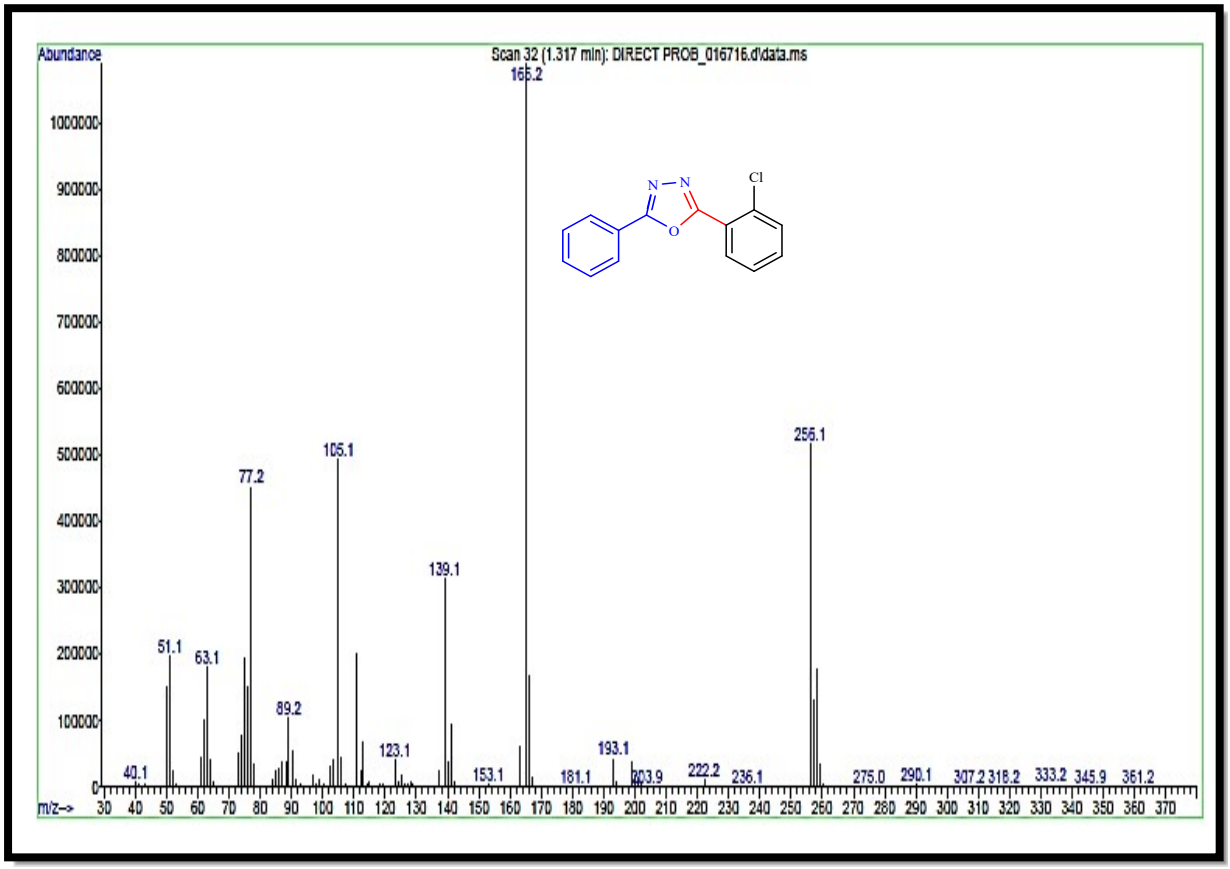
Abundance
Scan 32 (1.317 min): DIRECT PROB_016716.d\data.ms
165.2
256.1
105.1
77.2
139.1
51.1
63.1
89.2
123.1
193.1
40.1
153.1
181.1
203.9
222.2
236.1
275.0
290.1
307.2
318.2
333.2
345.9
361.2
m/z-->
N
N
O
Cl

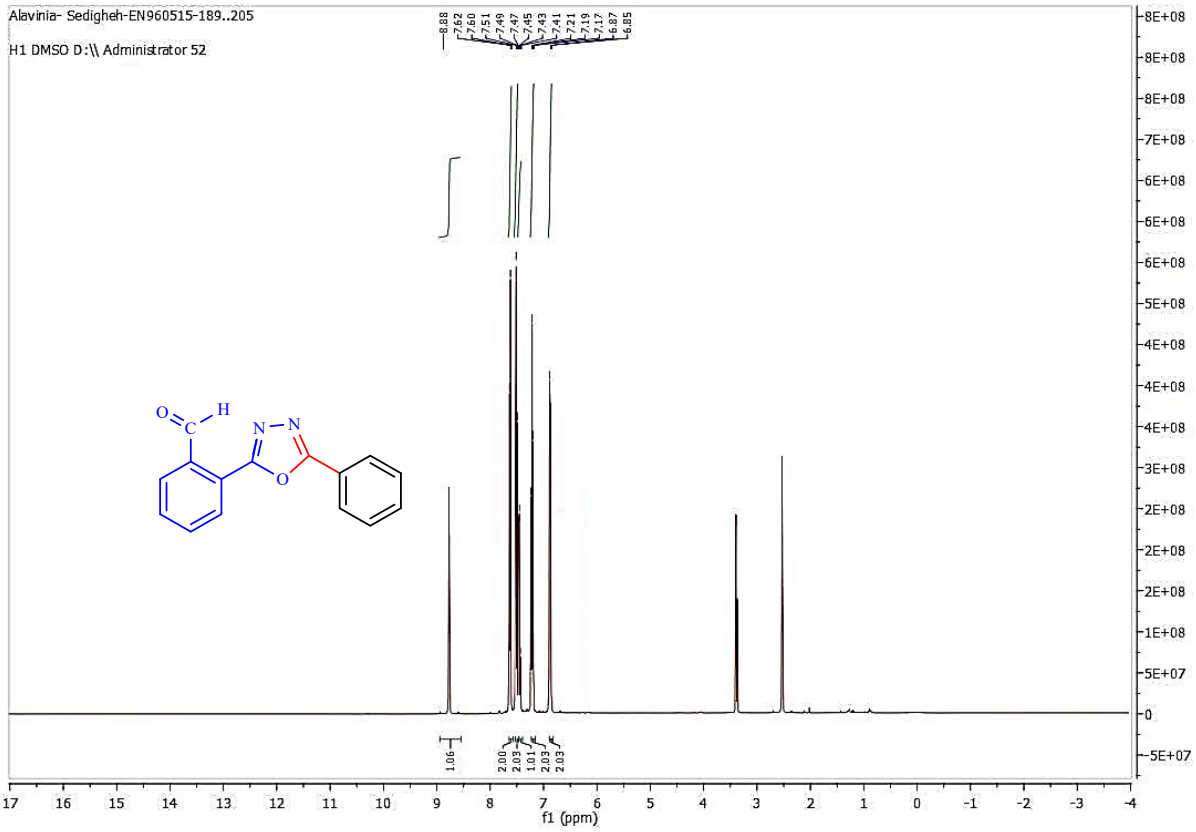
Alavinia- Sedigheh-EN960515-189..205
H1 DMSO D:\\ Administrator 52
8.88
7.62
7.60
7.51
7.49
7.47
7.45
7.43
7.41
7.21
7.19
7.17
6.87
6.85
1.06
2.00
2.03
1.01
2.03
2.03
f1 (ppm)

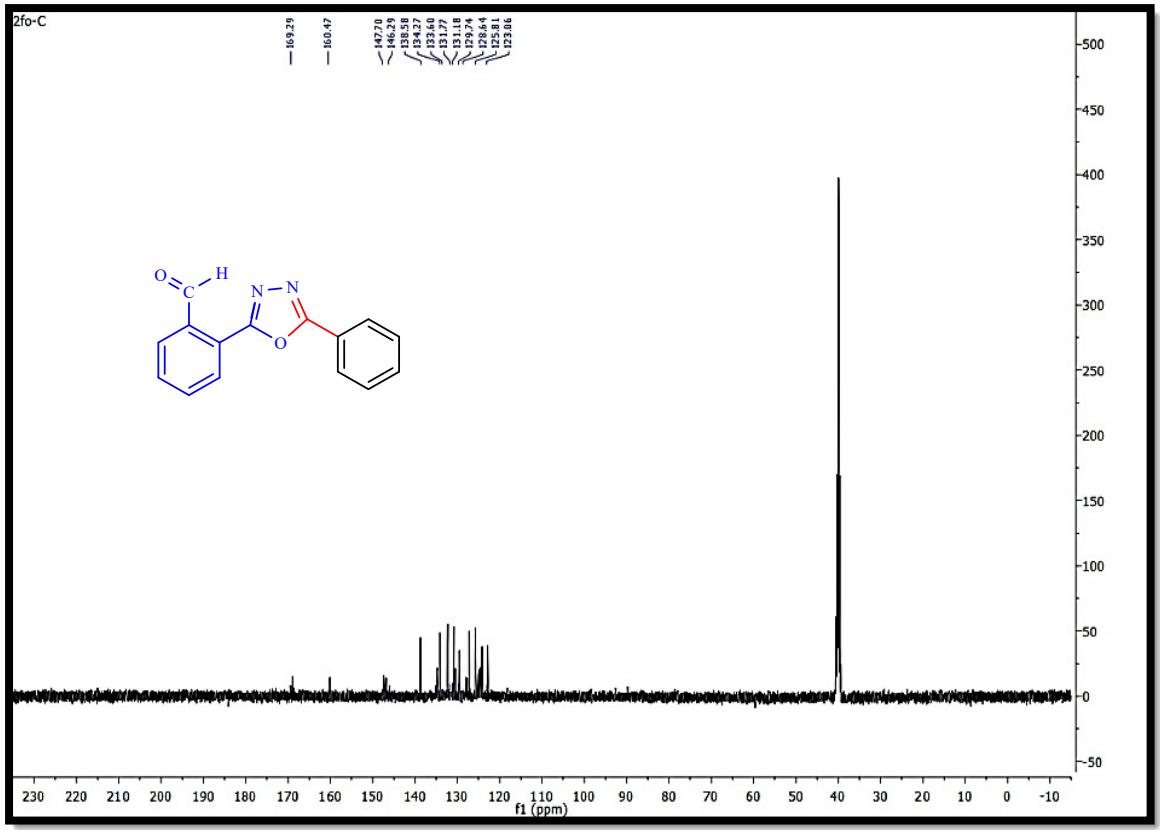
2fo-C
169.29
160.47
147.70
146.29
138.58
134.27
133.60
131.77
131.18
129.74
128.64
125.81
123.06
f1 (ppm)

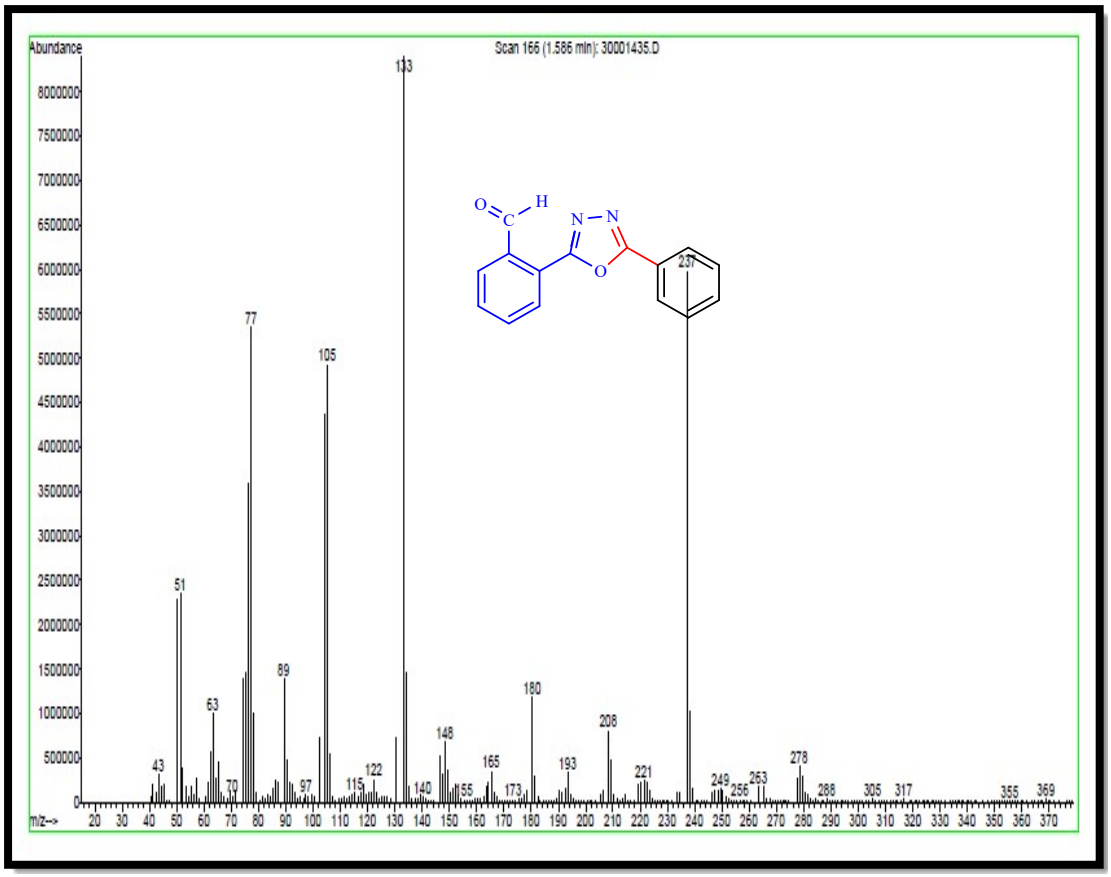
Abundance
Scan 166 (1.586 min): 30001435.D
133
77
105
51
89
63
43
180
208
148
165
193
221
278
237
m/z-->

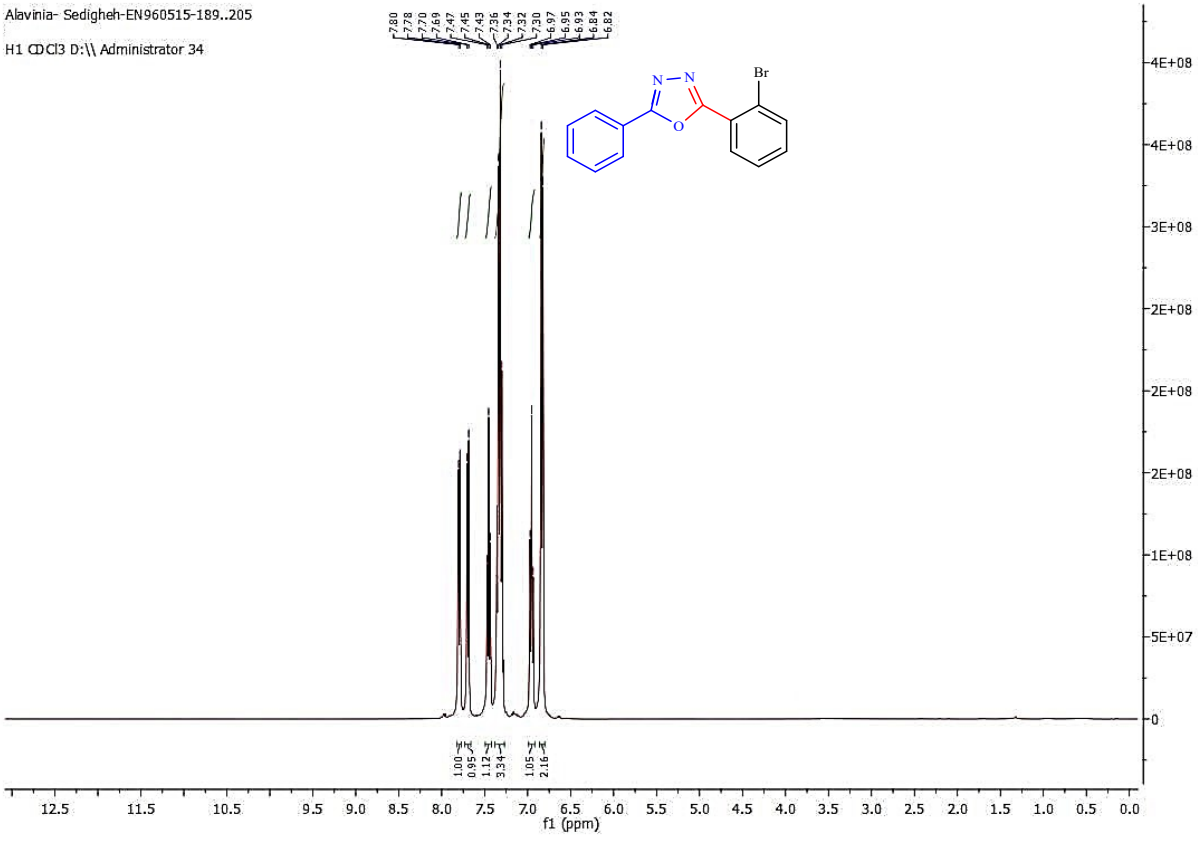
Alavinia- Sedigheh-EN960515-189..205
H1 CDCl3 D:\\ Administrator 34
Br
f1 (ppm)

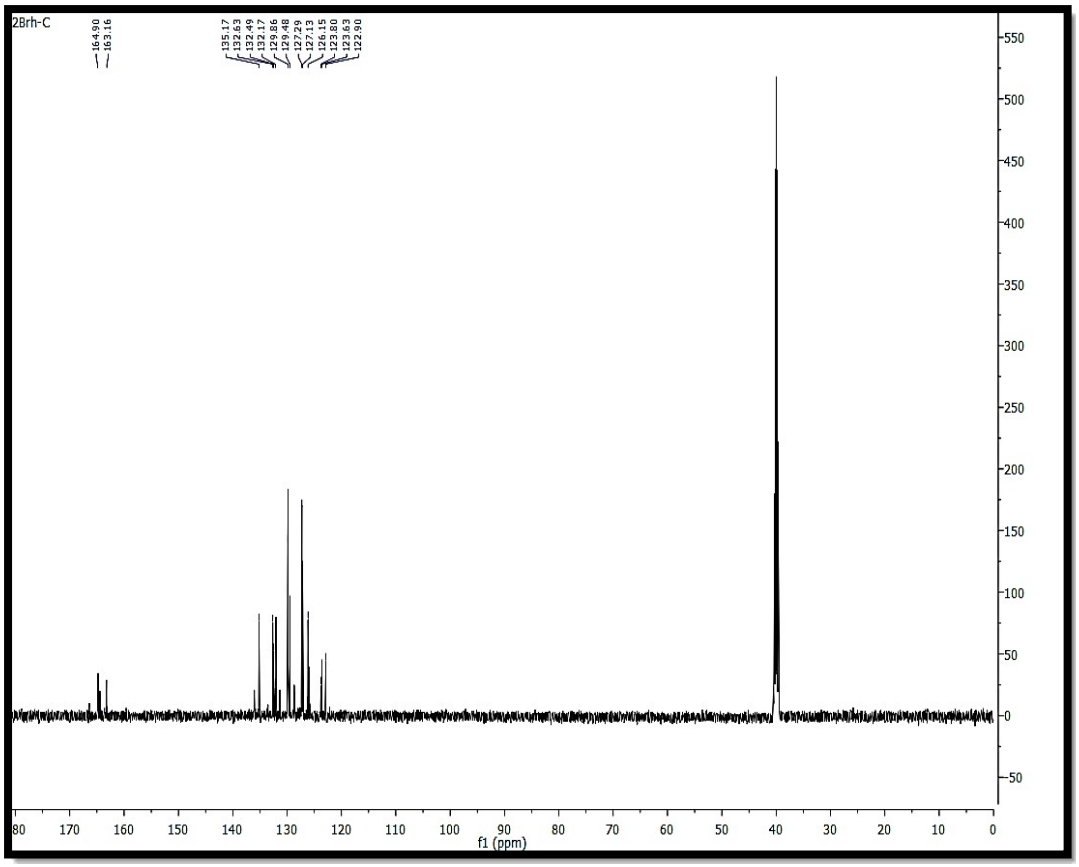
2Brh-C
164.90
163.16
135.17
132.58
132.49
132.17
129.86
129.48
127.29
127.13
126.15
123.80
123.63
122.90
f1 (ppm)

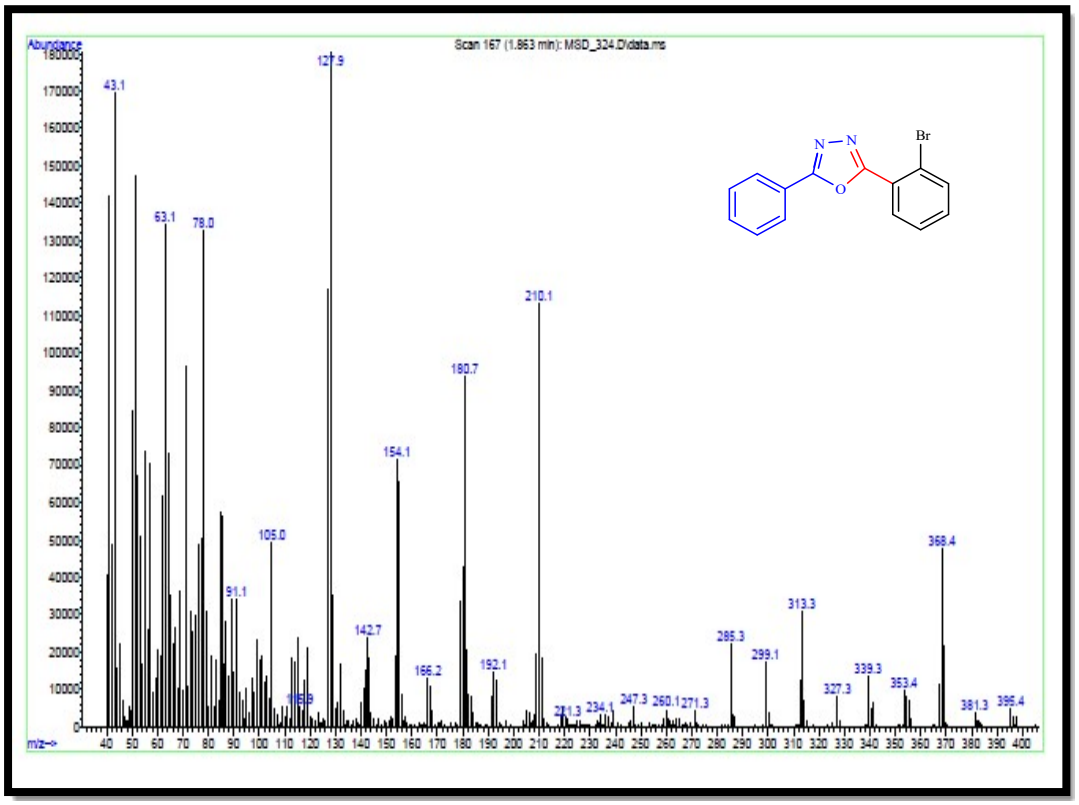
Abundance
Scan 167 (1.863 min): MSD_324.D\data.ms
m/z-->

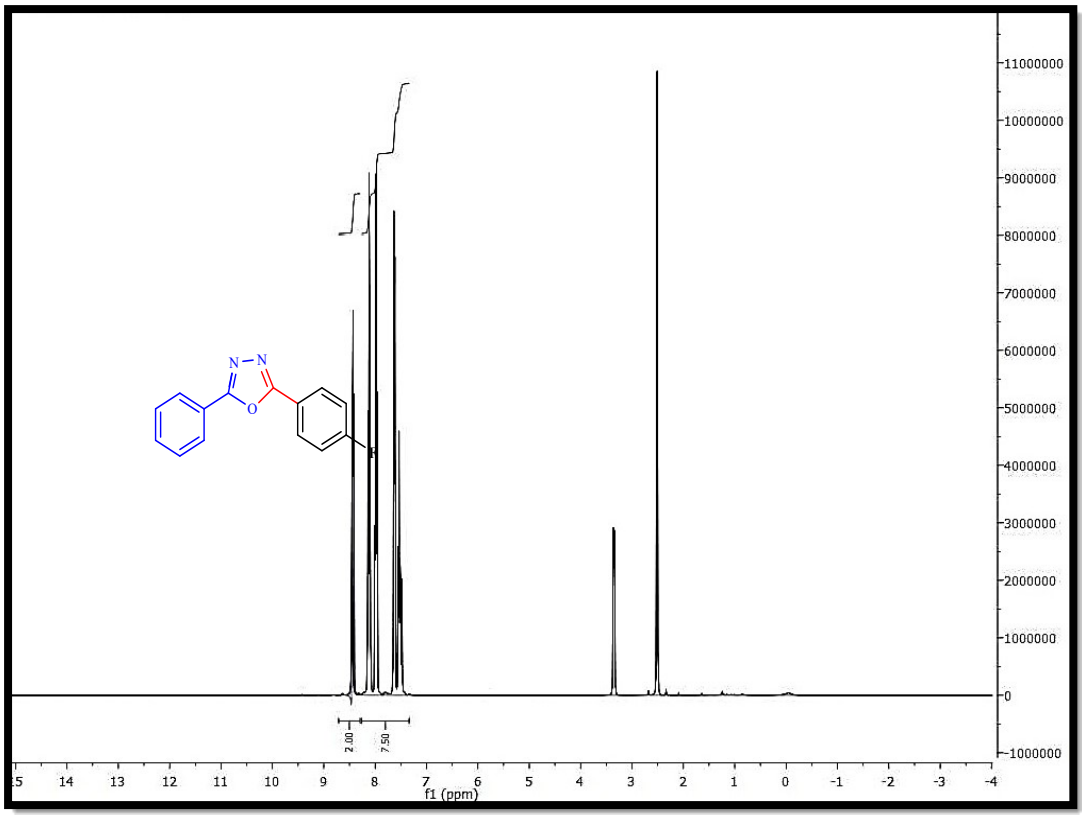
11000000
10000000
9000000
8000000
7000000
6000000
5000000
4000000
3000000
2000000
1000000
0
-1000000
2.00
7.50
f1 (ppm)


4F
C13e DMSO D:\\ Administrator
163.355
160.919
145.789
129.020
119.452
118.445
115.912
115.696
113.835
F
60000
50000
40000
30000
20000
10000
0
200
150
100
50
0


N
N
O
Cl
Cl
1.86
1.00
1.95
3.41
f1 (ppm)

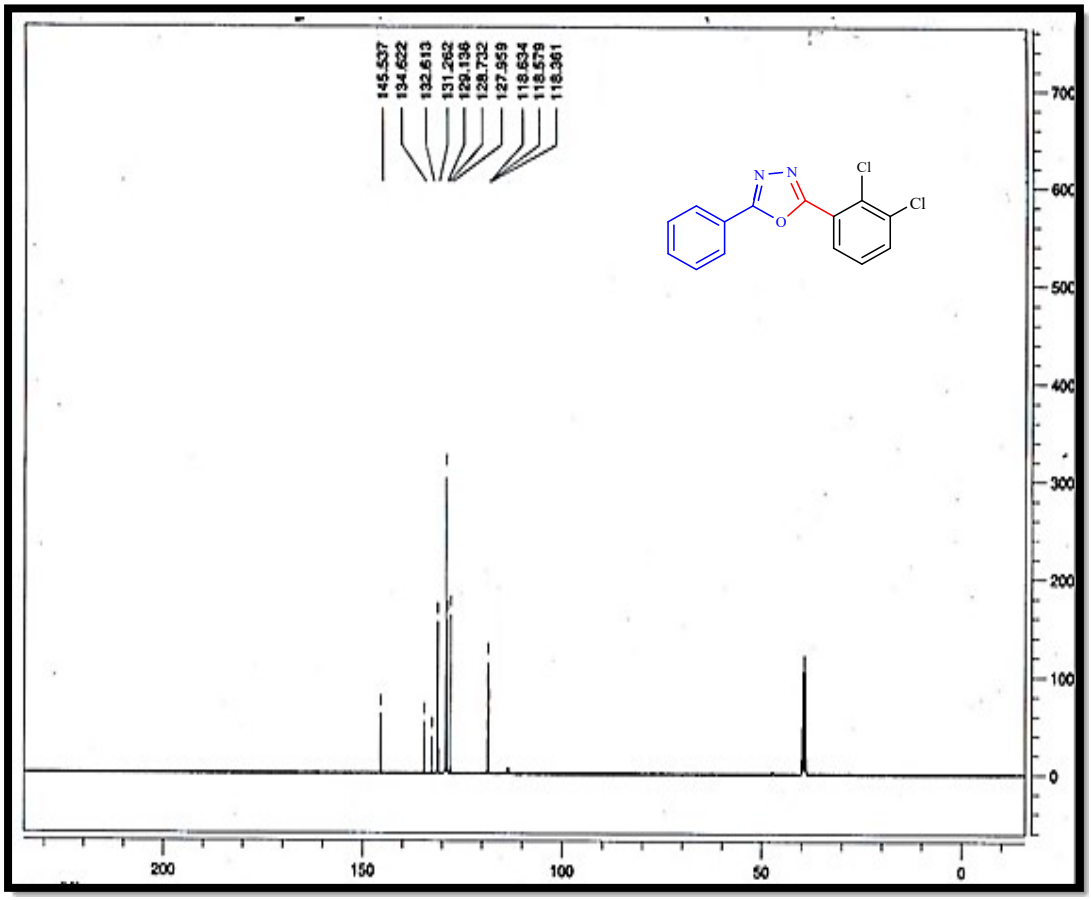
145.537
134.622
132.613
131.262
129.136
128.732
127.959
118.634
118.579
118.361
N
N
O
Cl
Cl

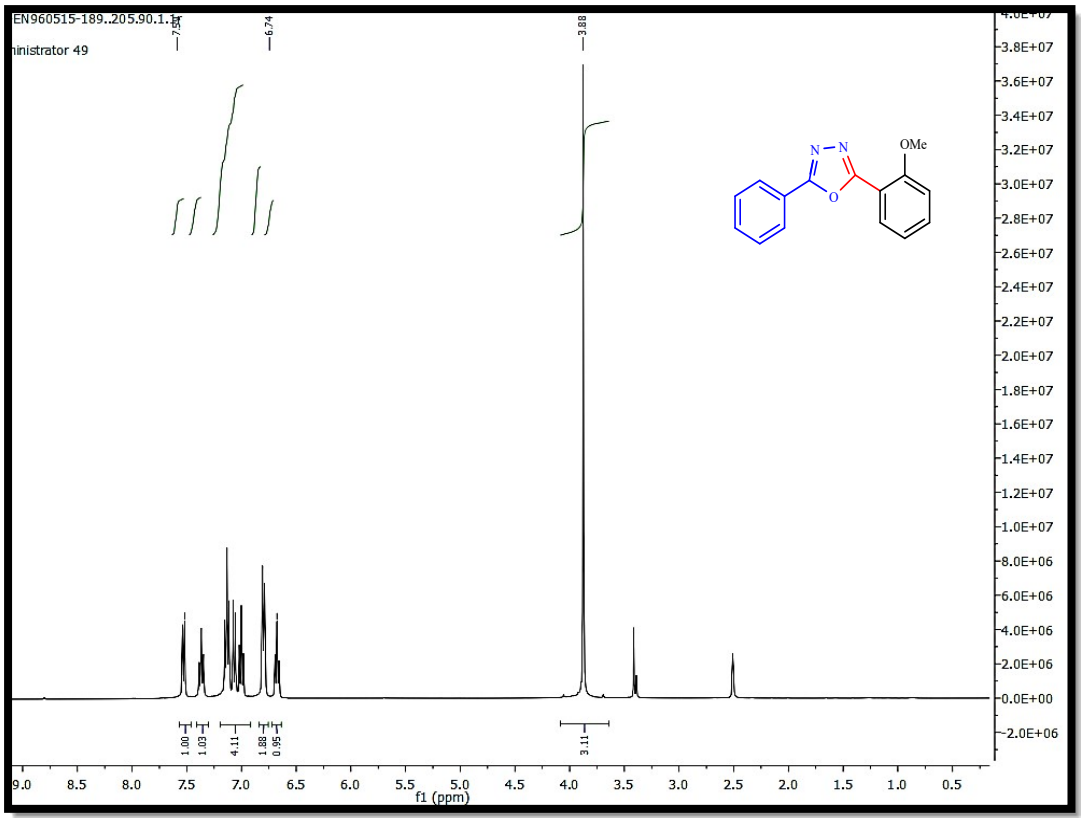
EN960515-189..205.90.1.1r
inistrator 49
7.54
6.74
3.88
OMe
N
N
O
1.00
1.03
4.11
1.88
0.95
3.11
f1 (ppm)

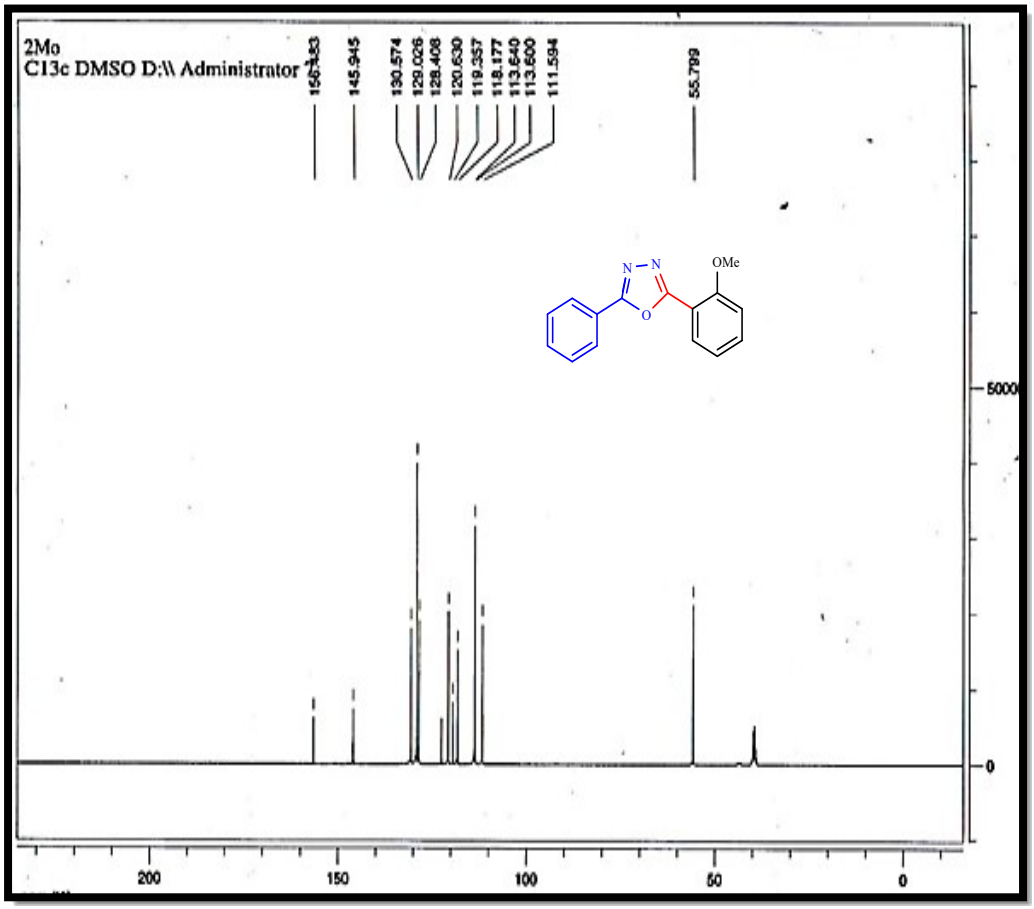
2Mo
C13c DMSO D:\\ Administrator
156.353
145.945
130.574
129.026
128.408
120.630
119.357
118.177
113.640
113.600
111.594
55.799
OMe
N
N
O
5000
0
200
150
100
50
0

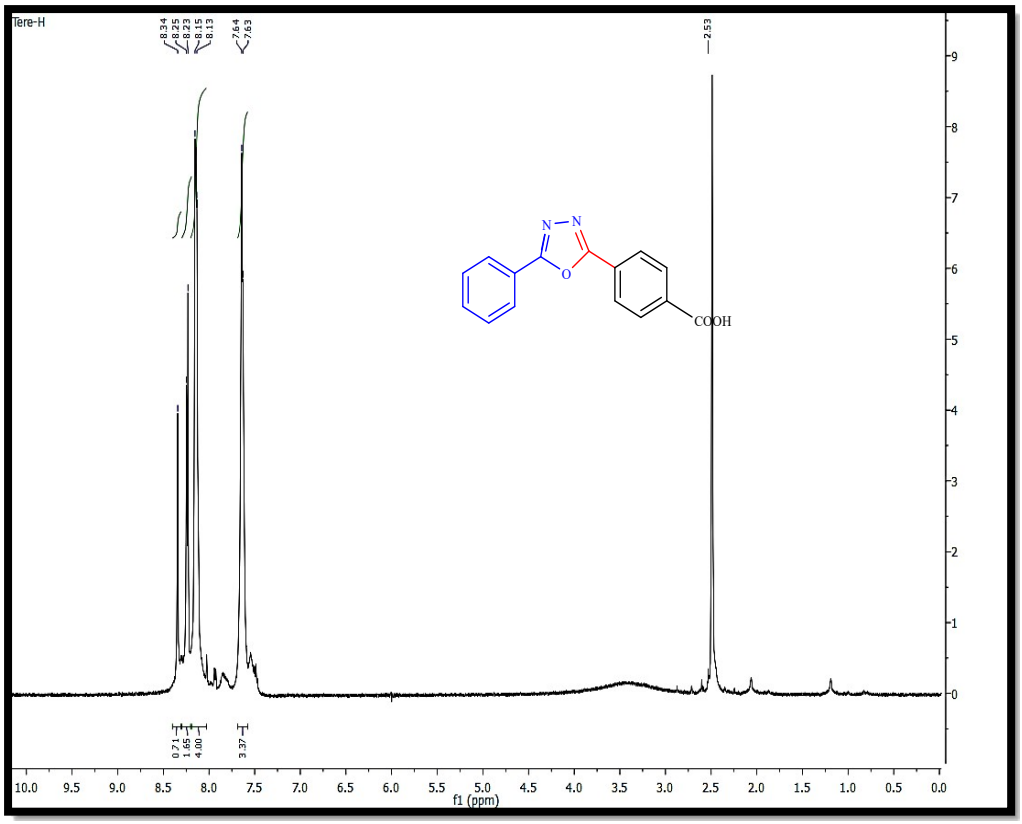
Tere-H
8.34
8.25
8.23
8.15
8.13
7.64
7.63
2.53
0.71
1.65
4.00
3.37
N
N
O
COOH
10.0
9.5
9.0
8.5
8.0
7.5
7.0
6.5
6.0
5.5
5.0
4.5
4.0
3.5
3.0
2.5
2.0
1.5
1.0
0.5
0.0
f1 (ppm)

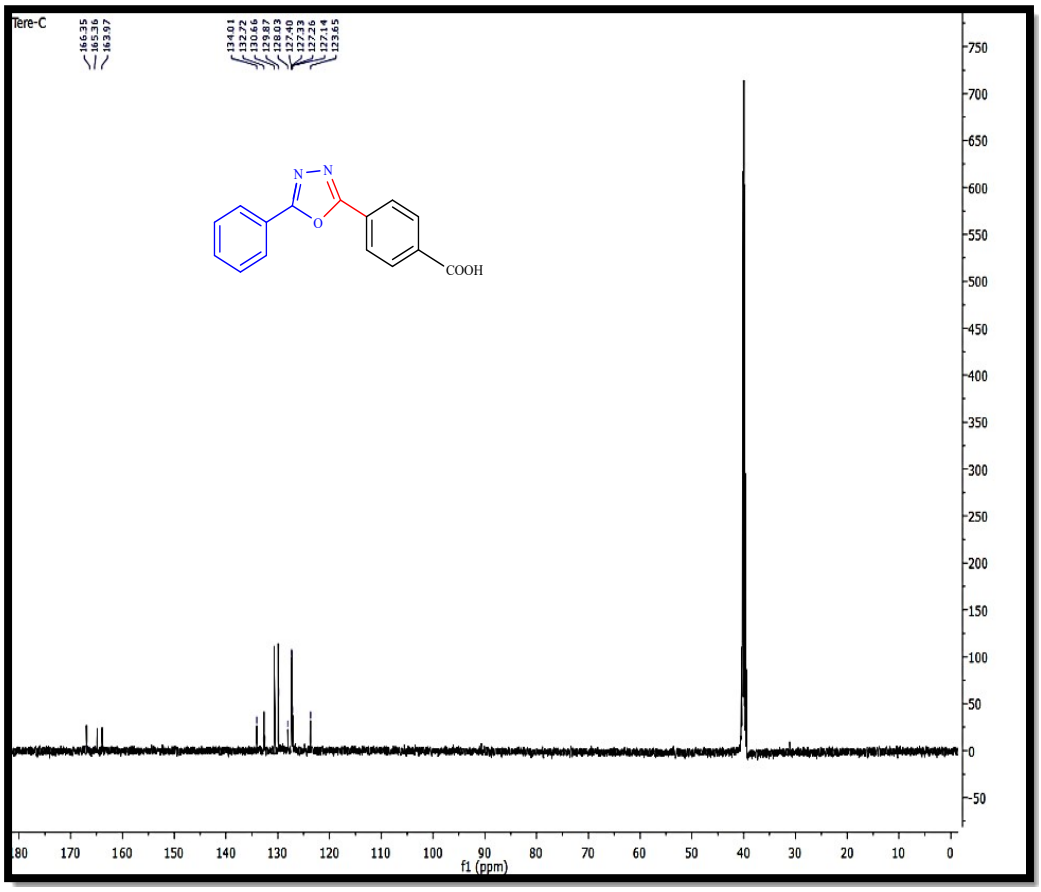
Tere-C
166.35
165.36
163.97
134.01
132.72
130.66
130.07
128.03
127.40
127.33
127.26
127.14
123.65
N
N
O
COOH
f1 (ppm)

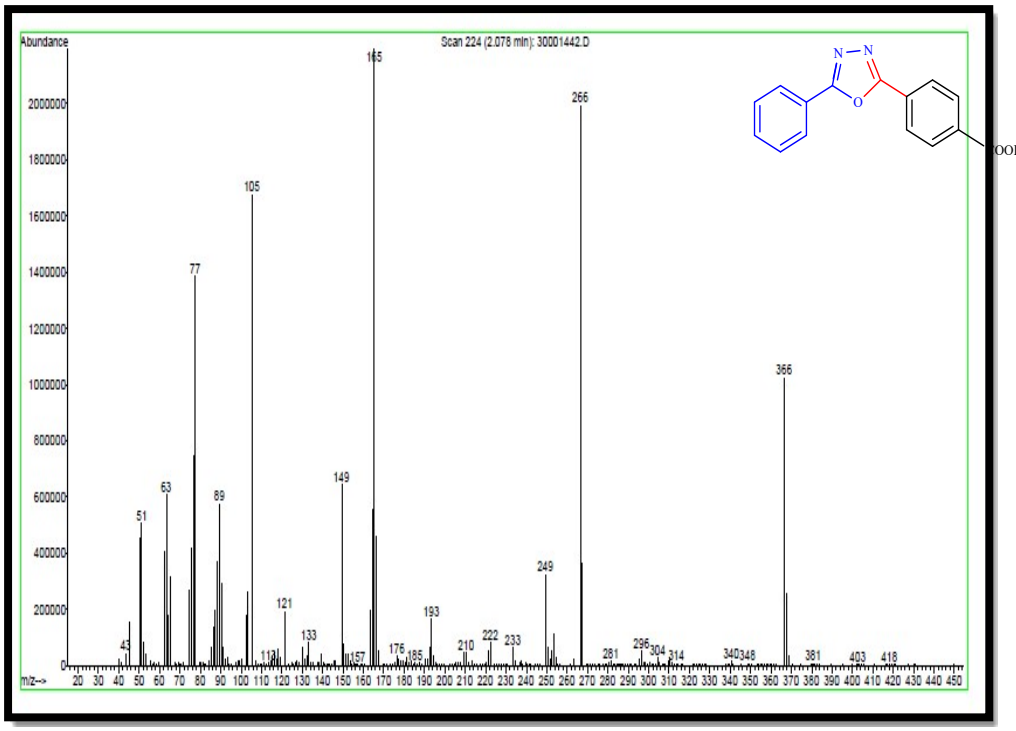
Abundance
Scan 224 (2.078 min): 30001442.D
m/z-->
N
N
O
OOH

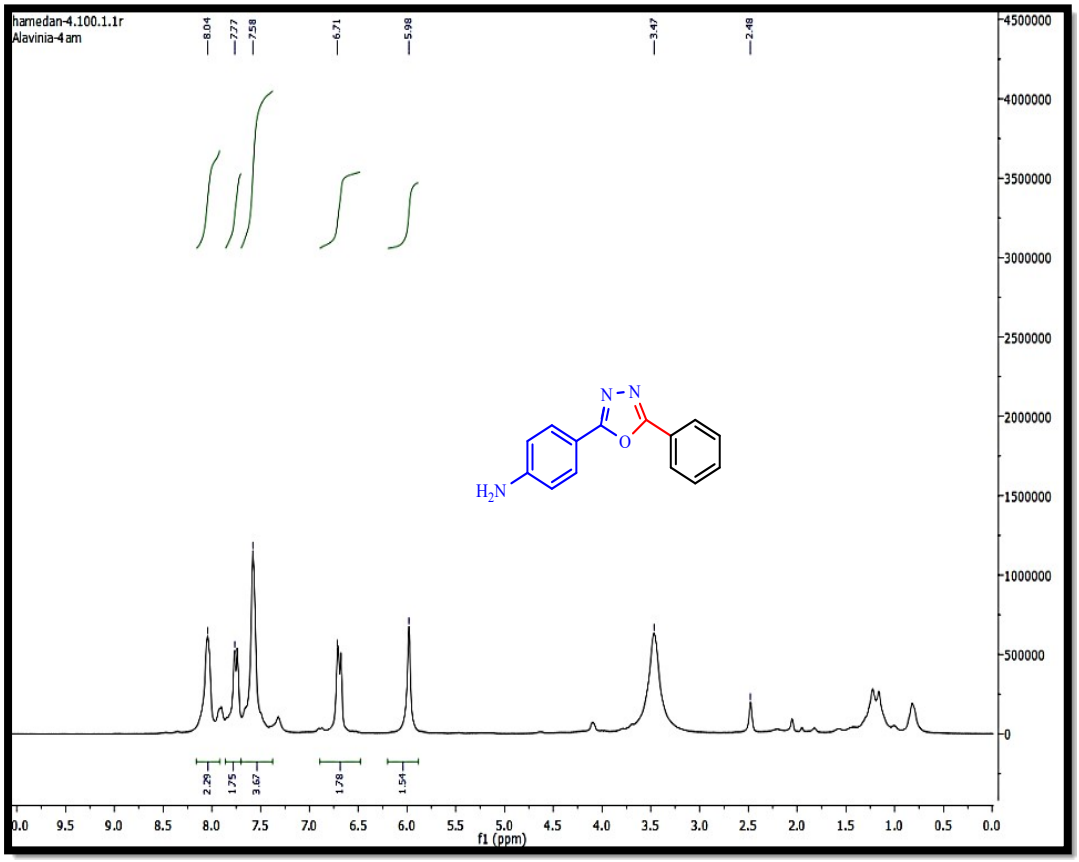
hamedan-4.100.1.1r
Alavinia-4 am
f1 (ppm)
N
N
O
H_2N

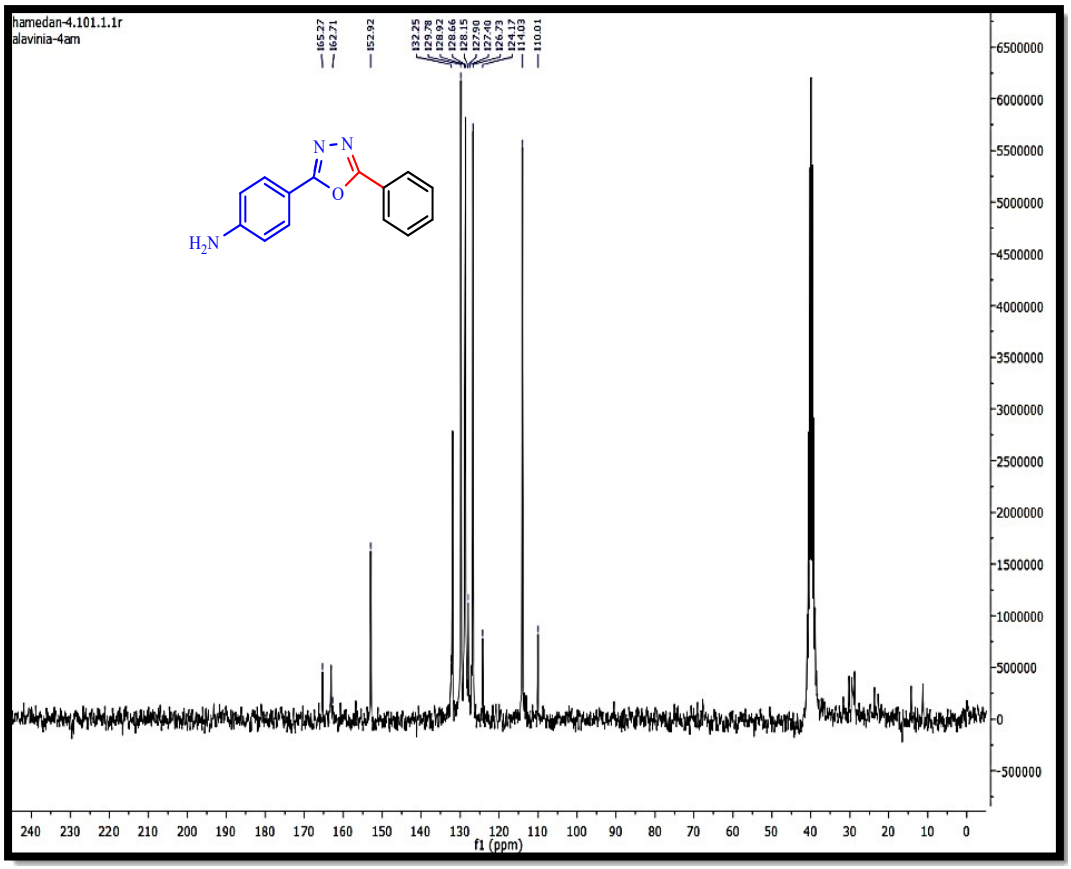
hamedan-4.101.1.1r
alavinia-4am
165.27
162.71
152.92
132.25
129.78
128.92
128.66
128.15
127.98
127.40
126.73
124.17
114.03
110.01
N – N
O
H_2N
f1 (ppm)

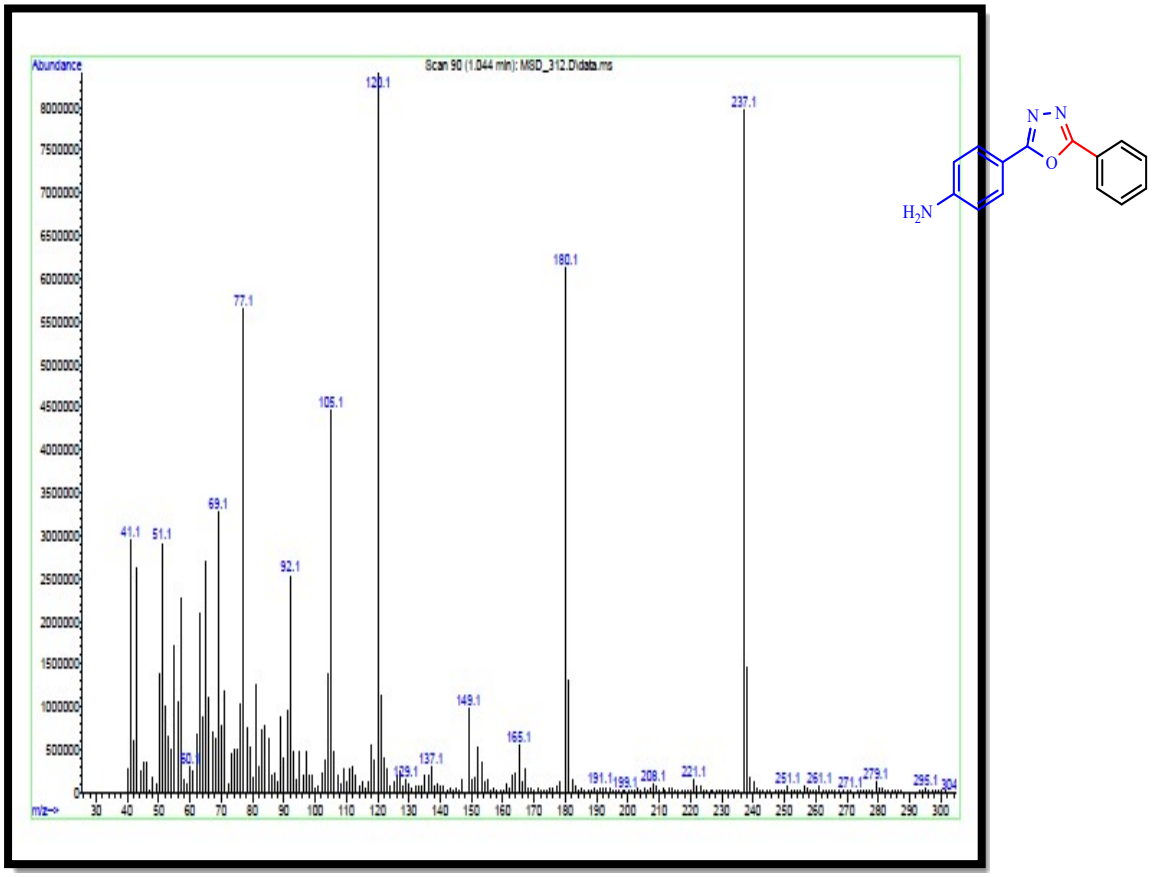
Abundance
Scan 90 (1.044 min): MSD_312.D\data.ms
120.1
237.1
180.1
77.1
105.1
69.1
41.1
51.1
92.1
149.1
165.1
137.1
129.1
191.1
196.1
208.1
221.1
251.1
261.1
271.1
279.1
295.1
304
m/z-->
N – N
O
H_2N

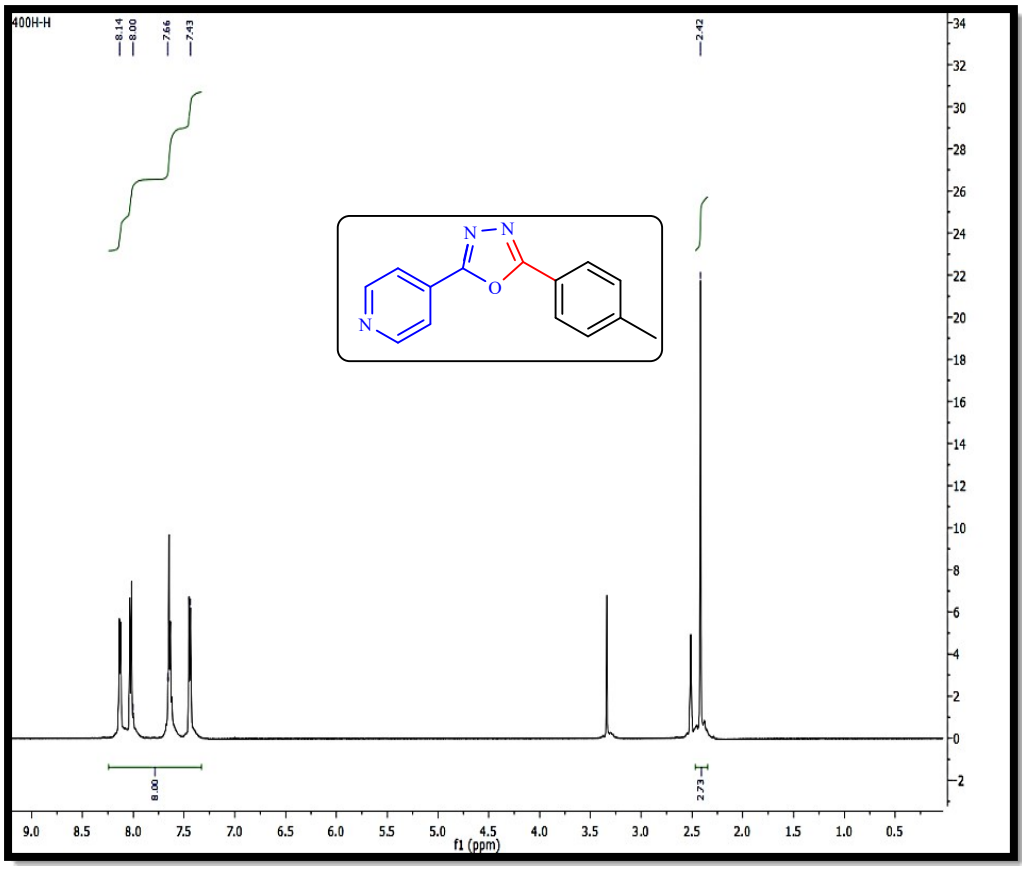
400H-H
8.14
8.00
7.66
7.43
2.42
8.00
2.73
f1 (ppm)

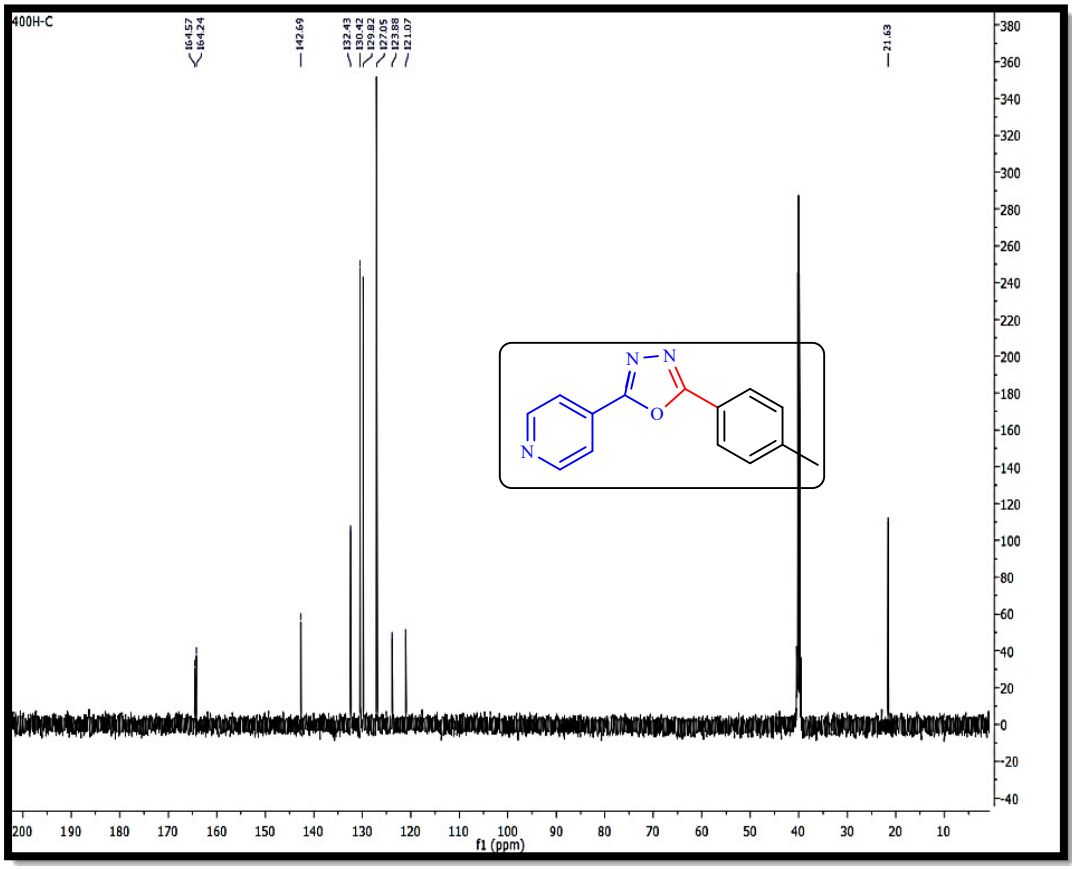
400H-C
164.57
164.24
142.69
132.43
130.42
129.82
127.05
123.88
121.07
21.63
f1 (ppm)